UNIVERSIDADE ESTADUAL DE CAMPINAS

INSTITUTO DE BIOLOGIA

AMARYLIS CLAUDINE BONITO AZEREDO WANSCHEL

"BIODISPONIBILIDADE CARDIOVASCULAR DO ÓXIDO NÍTRICO EM CAMUNDONGOS LDLR-/-"

Tese apresentada ao Instituto de Biologia para obtenção do Título de Doutora em Biologia Funcional e Molecular, na área de Fisiologia.

Marta H. Krieger

Orientadora: Profa. Dra. Marta Helena Krieger

Campinas, 2010

FICHA CATALOGRÁFICA ELABORADA PELA
BIBLIOTECA DO INSTITUTO DE BIOLOGIA – UNICAMP

W188b	Wanschel, Amarylis Claudine Bonito Azeredo Biodisponibilidade cardiovascular do óxido nítrico em camundongos LDLr-/- / Amarylis Claudine Bonito Azeredo Wanschel. – Campinas, SP: [s.n.], 2010. Orientadora: Marta Helena Krieger. Tese (doutorado) – Universidade Estadual de Campinas, Instituto de Biologia. 1. Óxido nítrico. 2. Endotélio. 3. Hipertrofia ventricular. 4. Hipercolesterolemia. 5. Estresse oxidativo. I. Krieger, Marta Helena. II. Universidade Estadual de Campinas. Instituto de Biologia. III. Título. (rcdt/ib)

Título em inglês: Cardiovascular bioavailability of nitric oxide in mice LDLr-/- mice.
Palavras-chave em inglês: Nitric oxide; Endothelium; Ventricle hypertrophy; Hypercholesterolemia; Oxidative stress.
Área de concentração: Fisiologia.
Titulação: Doutora em Biologia Funcional e Molecular.
Banca examinadora: Marta Helena Krieger, Edson Antunes, Dora Maria Grassie-Kassisse, Edilamar Menezes de Oliveira, Lusiane Maria Bendhack.
Data da defesa: 05/04/2010.
Programa de Pós-Graduação: Biologia Funcional e Molecular.

Campinas, 05 de Abril de 2010.

BANCA EXAMINADORA

Profa. Dra. Marta Helena Krieger (Orientadora) — Assinatura

Profa. Dra. Lusiane Maria Bendhack — Assinatura

Profa. Dra. Edilamar Menezes de Oliveira — Assinatura

Prof. Dr. Edson Antunes — Assinatura

Profa. Dra. Dora Maria Grassi Kassisse — Assinatura

Profa. Dra. Maria Cláudia Irigoyen — Assinatura

Profa. Dra. Helena Coutinho Franco de Oliveira. — Assinatura

Prof. Dr. Miguel Arcanjo Areas — Assinatura

DEDICO

Esta tese aos meus queridos irmãos, Thais Tatiana Bonito Wanschel, Ciro Douglas Bonito Wanschel e Priscila Luana Bonito Marin.

AGRADECIMENTOS

À minha orientadora, Profa Dra Marta Helena Krieger, meus agradecimentos por sua orientação, e por acreditar em meu trabalho para concluir essa tese.

Ao meu co-orientador, Prof. Heraldo Possolo de Souza pela dedicação e pelos ensinamentos.

À minha amiga e colaboradora Ana Iochabel Soares Moretti por sua sabedoria e seriedade científica e por ser sempre paciente e solícita.

À amiga e Professora Dra Dora Grassi Kassisse do Laboratório de Estresse pelo carinho e ajuda.

À Profa Dra Regina Spadari-Bratfish do laboratório de Biociências meus agradecimentos especiais por sua orientação e pela pontualidade.

Aos meus pais Tito Cláudio Wanschel e Vera Lúcia Mendes Bonito Wanschel pelo carinho e incentivo aos estudos.

Ao meu companheiro de todas as horas Alessandro Gonzalez Salerno meus agradecimentos especiais por seu apoio científico, intelectual e pelo amor e carinho.

Às minhas amigas de laboratório e departamento Viviane de Menezes Cáceres, Emiliane Miguel Salomão e Claudia Yano que contribuíram direta ou indiretamente com informações técnicas, diversão e amizade.

A todos os amigos de trabalho, do curso de pós-graduação que contribuíram cientificamente durante todo desenvolvimento desta tese ajustando protocolos, emprestando materiais e discutindo resultados.

Aos funcionários do departamento de Fisiologia e Biofísica Léscio Teixeira e Marcelo Duque pela seriedade e competência profissional.

Aos funcionários da secretaria da pós-graduação Andréia Aparecida Vigiliato, Sílvia e Rafael pela eficiência e bom humor.

À Coordenação de Aperfeiçoamento de Pessoal de Nível Superior (CAPES), ao Conselho Nacional de Desenvolvimento Científico e Tecnológico (CNPq) e à Fundação de Amparo à Ciência e Tecnologia do Estado de São Paulo (FAPESP), pelo apoio financeiro.

LISTA DE ABREVIATURAS

Ach acetilcolina

ADMA dimetil arginina assimétrica

AngII angiotensina-2

ANOVA análise de variância

AKT/ PI3K protein kinase B/phosphoinoside-3-kinase

ApoE apolipoproteína E

B_1AR betadrenoceptor-1

β_2AR betadrenoceptor-2

BST biotin-switch

BSA albumina de soro bovino

BH4 tetrahidrobiopterina

C camundongos LDLr-/- alimentados com dieta comercial por 15 dias

C15 camundongos LDLr-/- alimentados com dieta comercial por 15 dias

C30 camundongos LDLr-/- alimentados com dieta comercial por 30 dias

C60 camundongos LDLr-/- alimentados com dieta comercial por 60 dias

Caspase cysteine-aspartic-acid-proteases

CaM calmodulina

CG guanilato ciclase

CHIP c-terminal HSP70-interactin protein

CMLs células musculares lisas

DCV doenças cardiovasculares

DHE dihidroetidina

DTPA diethylenetriamine pentaacetic acid

GMPc guanosina mono-fosfato cíclica

E etídio

EDRF fator de relaxamento derivado do endotélio

EOH 2-hidroxietídio

eNOS óxido nítrico sintase endotelial

EPM erro-padrão da média

ERKs quinases de regulação extracelular

EROs espécies reativas de oxigênio

ET1 endotelina 1

FAD dinucleotídeo flavina adenina

FMN mononucleotídeo flavina

GAPDH glyceraldehyde 3-phosphate dehydrogenase

Gi proteína G inibitória

GMPc guanosina monofosfato cíclica

Gs proteína estimulatória

GSH glutationa

GSNO S-nitrosoglutationa

H camundongos LDLr-/- alimentados com dieta hiperlipidêmica + ácido cólico por 15 dias

H15 camundongos LDLr-/- alimentados com dieta hiperlipidêmica por 15 dias

H30 camundongos LDLr-/- alimentados com dieta hiperlipidêmica por 30 dias

H60 camundongos LDLr-/- alimentados com dieta hiperlipidêmica por 60 dias

H + S camundongos LDLr-/- alimentados com dieta hiperlipidêmica + SNAC por 15 dias

HMG-CoA redutase 3-hydroxy-3-methyl-glutaryl-CoA redutase

H_2O_2 peróxido de hidrogênio

HRP enzyme horseradish peroxidase

HPLC high performance liquide chromatography

HSP90 heat shock protein 90

HSP70 heat shock protein 70

HVE hipertrofia ventricular esquerda

IL-8 interleucina 8

iNOS óxido nítrico sintase induzível

ISO isoprenalina

LDL lipoproteína de baixa densidade

LV left ventricle

M molaridade

MAP quinases quinases ativadas por mitógenos

MG miligrama

MIP-1α proteína inflamatória de macrófago alfa

MMHG milímetro de mercúrio

MPB n-(3-maleimidylpropionyl) biocytin

N número de observações experimentais

NEM N-ethylmaleimide

nNOS óxido nítrico sintase neuronal

NAD dinucleotídeo da nicotinamida adenina

NADPH dinucleotídeo da nicotinamida adenina (fosfato)

NF-Kb fator nuclear de transcrição kB

$NO^{\bullet}$ óxido nítrico

NO^-_2 nitrito

NO^-_3 nitrato

NOSc óxido nítrico sintase constitutiva

NOSIP "nitric oxide synthase intreracting protein"

NOSTRIN "nitric oxide synthase traffic inducer"

NPS nitroprussiato de sódio

NS não significativo

NT nitrotirosina

O_2^- ânion superóxido

$OH^\bullet$ radical hidroxila

$ONOO^-$ peroxinitrito

PMSF phenylmethylsulfonyl fluoride

PBS phosphate-buffered saline

PKGI proteína quinase 1

RPM rotações por minuto

RSH tióis

RT room temperature

S1179 resíduo de serina 1179

SEM erro padrão da média

Ser serina

SDS dodecil sulfato de sódio

SHR ratos esponaneamente hipertensos

SNAC s-nitroso-n-acetilcisteína

SNAP s-nitroso-n-acetilpenicilamina

SNO nitrosotiol

SOD superóxido dismutase

TBS tris-HCl-buffered saline

TBST tris-HCl-buffered saline + Tween-20

TG triglicérides

TNFα- Fator de necrose tumoral alfa

Tris (hydroxymethyl) aminomethane

TUNEL terminal deoxynucleotidyl transferase dUTP nick end labeling

VCL3 vanadium trichloride

SUMÁRIO

RESUMO

O objetivo deste trabalho foi avaliar a biodisponibilidade do óxido nítrico ($NO^{\bullet}$) nas disfunções cardiovasculares, especificamente na hipertrofia ventricular esquerda e na aterosclerose. Para tanto, realizamos dois estudos em camundongos deficientes do receptor de LDL (LDLr-/-): o primeiro realizado em continuidade aos estudos desenvolvidos anteriormente em nosso grupo de pesquisa, os quais demonstraram a ação do doador de $NO^{\bullet}$ na prevenção da hipertrofia ventricular esquerda e na proteção contra arritmia via indução do acoplamento adrenoceptor-beta2 (β_2AR) à proteína G inibitória (Gi); e no segundo estudo, foi avaliada a biodisponibilidade de $NO^{\bullet}$ na fase inicial da aterogênese, com objetivo de caracterizar as alterações sistêmicas e locais. No primeiro estudo mostramos que o doador de $NO^{\bullet}$, S-Nitroso-N-acetilcisteína (SNAC) administrado, promoveu ação cardioprotetora contra o remodelamento cardíaco via redução do estresse oxidativo e apoptose celular, os quais foram determinados pelas medidas ventriculares da produção de superóxido ($O^{-\bullet}_2$) e peróxido de hidrogênio (H_2O_2) e pelo índice de morte celular por apoptose. Esta ação cardioprotetora foi vista no aumento da expressão e no conteúdo de S-nitrosação do β_2AR. Estes efeitos foram associados à cardioproteção contra a arritmia via indução do acoplamento β_2AR à Gi. O objetivo do segundo estudo foi avaliar a biodisponibilidade de $NO^{\bullet}$ na fase inicial da aterogênese em camundongos LDLr-/- no curso temporal de 15 a 60 dias de dieta, com a quantificação de parâmetros sistêmicos representados pela pressão arterial, perfil lipidêmico e ateroma, bem como de parâmetros locais representados pela atividade e expressão da via NO/NOS e suas modificações pós-traducionais no processo inflamatório via CD40-CD40L. Camundongos LDLr-/- submetidos à dieta rica em gordura apresentaram progressão do tamanho do ateroma no

curso temporal analisado, contudo não foi associado a similares incrementos nos níveis de dislipidemia. Não foram detectadas alterações na pressão arterial do fenótipo hipertenso deste animal. Contudo, localmente foi verificado incremento na atividade da eNOS via fosforilação de resíduos de serina 1179 (S1179) em 30 dias de dieta rica em gordura, que pode ser considerado um mecanismo emergencial à aterosclerose . Posteriormente, com a evolução do ateroma (60 dias) houve redução desta ativação, bem como do conteúdo de proteínas S-nitrosadas. O desenvolvimento de ateroma em 30 e 60 dias induzido pela dieta mostrou aumento da atividade inflamatória por meio da denitrosação de tióis críticos da via CD40. Portanto, a análise das alterações no curso temporal apresentou somente mudanças locais como alteração na biodisponibilidade de $NO^{\bullet}$, ativação inflamatória via denitrosação do receptor CD40 e redução do conteúdo de S-nitrosação total, enquanto as alterações sistêmicas neste período de tempo ainda não são evidentes.

ABSTRACT

The objective of this study was to evaluate the bioavailability of nitric oxide ($NO^{\bullet}$) in cardiovascular disorders, specifically on the left ventricular hypertrophy and atherosclerosis. Therefore, we performed two studies with LDL receptor-deficient mice (LDLr-/-): the first one was performed in sequence to the studies previously developed in our research group, which showed the $NO^{\bullet}$ donor action on the prevention of left ventricular hypertrophy and protection against arrhythmia via induction of the coupling from beta adrenoceptor-2 (β_2AR) to the inhibitory G protein (Gi); and the second study,it was evaluated the bioavailability of $NO^{\bullet}$ to characterize the systemic and local alterations in the early stages of atherogenesis. The first study showed that the administration of $NO^{\bullet}$ donor S-Nitroso-N-Acetylcysteine (SNAC) promoted cardioprotective action by blocked the cardiac remodeling through reduction of oxidative stress and of apoptosis, which were determined by measures of ventricular superoxide ($O^{-\bullet}_2$) and hydrogen peroxide (H_2O_2) production and the cell death index, respectively. This cardiprotective action was charactherized by the increase of expression and content of S-nitrosation of β_2AR. These effects were associated with cardioprotection against arrhythimia via induction of β_2AR coupling Gi. The objective of the second study was to evaluate the bioavailability of $NO^{\bullet}$ in the LDLr-/- mice early atherogenesis in LDLr-/ - mice from 15 to 60 days, with the quantification of systemic parameters represented by the blood pressure, lipidemic profile and atheroma as well as local ones represented by the activity and expression of NO/NOS pathway and its post-translational modifications on the inflammatory process via CD40-CD40L. Mice LDLr-/ - maintained on high-fat diet showed progression of atheroma size, although it was not associated with similar increase in dyslipidemic profile. No changes in

blood pressure were detected in the hypertensive phenotype of this animal. However, increased activity of eNOS via phosphorylation of Ser1179 (S1179) at 30 days of high-fat diet was detected and it can be considered an emergential mechanism to early atherosclerosis. The development of atheroma (60 days) blocked that activation as well as the protein content of S-nitrosated. The atheroma induced at 30 and 60 days by high-fat diet revealed increase inflammatory activity through denitrosation of critical thiols via CD40. Therefore, the analysis of changes in this time course showed only local changes as changes on $NO^{\bullet}$ bioavailability alteration inflammatory activation via denitrosation of CD40 receptor and the content of total S-nitrosation reduction. However, systemic changes in this period of time have not been evident yet.

I - INTRODUÇÃO

"O impacto das doenças cardiovasculares sobre a morbidade e mortalidade no mundo vem crescendo em grandes proporções. Enquanto no início do século XX as doenças cardiovasculares (DCV) representavam menos que 10% das mortes em todo mundo, no início do século XXI passaram a representar cerca de metade de todas as mortes no mundo desenvolvido e 25% no mundo em desenvolvimento. O fato é o de que, durante o último século, as DCV se tornaram a principal causa de mortalidade e morbidade. Em consequência disso, estima-se que as atuais 15 milhões de mortes anuais, em 2020 passem a ser 25 milhões por ano, superando as doenças infecciosas" (WHO – World Health Report 2002 apud Krieger, p.415).

Na base da maioria das doenças cardiovasculares encontra-se a doença vascular, especialmente a aterosclerose, que se manifesta em "algum grau" em todos os adultos e que tem como principais manifestações clínicas a doença arterial coronariana, o infarto cerebral e as arteriopatias periféricas (Libby, *et al.,* 2005). Múltiplos fatores de risco como tabagismo, dislipidemias, hipertensão arterial sistêmica, resistência insulínica e *diabetes mellitus*, obesidade e sedentarismo podem promover uma disfunção endotelial aumentando a susceptibilidade à aterosclerose. A disfunção do endotélio é caracterizada pela significativa diminuição à resposta vasodilatadora, promovida principalmente pelo composto vasoativo de maior relevância-óxido nítrico ($NO^{\bullet}$), bem como pelo aumento a resposta vasoconstritora (Lerman, *et al.,* 1992).

1- Biodisponibilidade do Óxido Nítrico ($NO^{\bullet}$) no Sistema Cardiovascular

O óxido nítrico é um radical livre, gasoso, inorgânico, incolor, que apresenta um elétron desemparelhado na última camada e uma meia vida de 4 a 8 segundos em meio

aquoso oxigenado (Moncada *et al.*, 1989; Kojda *et al.,* 1999). Até meados da década de 1980, o $NO^{\bullet}$ era considerado apenas membro de uma família de poluentes ambientais indesejáveis e potenciais carcinógenos. Nos últimos 30 anos, o $NO^{\bullet}$ tem sido considerado a molécula sinalizadora chave na via de transdução de sinal e isso ocorre em diversos tipos celulares que estão envolvidos em uma série de funções fisiológicas, como a neurotransmissão, citotoxicidade de macrófagos e modulação do sistema cardiovascular. Ele é um importante mediador de processos intra e extracelulares, uma vez que se difunde facilmente através das membranas biológicas (Palmer *et al.*, 1987).

O $NO^{\bullet}$ é biologicamente produzido pela família das enzimas NO sintases (NOS) (Napoli e Ignarro, 2001; Napoli, 2006), das quais três principais isoformas, codificadas em cromossomos e genes separados, têm sido identificadas em seres humanos e outros organismos (Napoli, 2006):

a) NOS neuronal (nNOS) expressa em certos neurônios, músculo esquelético, músculo liso e cardiomiócitos;

b) NOS induzível (iNOS) expressa por linhagens de células macrófagos/monócitos.

c) NOS endotelial (eNOS) expressa em células endoteliais e cardiomiócitos;

As três isoformas das NOS tem mecanismos enzimáticos similares que envolvem transferência de elétrons para oxidação do nitrogênio terminal da guanidina da L-arginina. Essas enzimas requerem inúmeros cofatores para função própria, incluindo tetrahidrobiopterina (BH4), nicotinamida-adenina-nucleotídeo fosfato (NADPH), dinucleotídeo flavina adenina (FAD) e mononucleotídeo flavina (FMN) (Alderton *et al*., 2001).

A nNOS é aquela presente nos gânglios nervosos intracardíacos, nas fibras nervosas atriais e em algumas fibras nervosas perivasculares dos ventrículos (Klimaschewski *et al.,* 1992). Sua expressão também foi detectada nos cardiomiócitos e nas células da musculatura lisa de pequenas e grandes artérias coronarianas de ratos e camundongos (Tambascia *et al.*, 2000; Krieger *et al*., 2006).

A iNOS é induzida por estímulo imunológico ou inflamatório. O coração adulto não expressa normalmente iNOS. Essa isoforma é ativada por mediadores do processo inflamatório em células endoteliais e cardiomiócitos (Andrew *et al.*, 1999). Em tais condições foi identificada no citosol (Kempf e Wollert, 2004), mas já foi encontrada no espaço perinuclear, no aparelho de Golgi, na mitocôndria e na membrana plasmática (Xu *et al.*, 2003)

A eNOS, encontrada principalmente nas células endoteliais em compartimentos denominados cavéolas (Shaul *et a.l*, 1998), é essencial para a manutenção do tono vascular basal. Também expressa no miocárdio sadio, a eNOS encontra-se principalmente no endotélio vascular coronariano e cardíaco (Shulz *et al*, 1991), bem como nos próprios cardiomiócitos (Ballingand *et al*, 1995). Nos cardiomiócitos, a eNOS encontra-se ancorada nas cavéolas por meio da proteína caveolina-3 da membrana plasmática, próximo aos canais de Ca^{+2} tipo L. Enquanto que a eNOS da vasculatura encontra-se ancorada nas cavéolas endoteliais por meio da proteína caveolina 1. A atividade da eNOS é bem caracterizada no ambiente vascular e é regulada por diferentes mecanismos após a sua tradução: inclusão de lipídios, mecanismo cálcio/calmodulina dependente, interações diretas proteína-proteína, diferentes fosforilações sítio dirigidas, glicosilação e disponibilidade de substratos e cofatores (Sessa, 2004). Assim, a eNOS pode interagir com

várias proteínas em seus estados “menos ativos” ou “mais ativos”. Para sua ativação são requeridas etapas de N-miristoilação e palmitoilação da eNOS ligada ao plasmalema, que no estado basal encontra-se associada à caveolina-1 e à proteína HSP 90. A proteína que faz interação com a HSP 70, denominada “CHIP”, interage com ambas HSP70 e HSP90 e regula negativamente o tráfego da eNOS para o complexo de Golgi, em contraste com a “NOSIP” e a “NOSTRIN” que podem “regular negativamente” a localização da eNOS na membrana plasmática.

O principal mecanismo de ativação da eNOS se dá pela fosforilação por meio da enzima Akt kinase (proteína kinase B), o que aumenta a sensibilidade da eNOS às concentrações basais de Ca^{++}/calmodulina (Fulton *et al.,* 1999). Contudo, são conhecidos cinco sítios de fosforilação da eNOS que modificam a sua atividade. Assim, esta isoforma pode ser fosforilada em vários resíduos de serina e treonina (Dudzinski *et al.*, 2006; Boo *et al*., 2003), destes potenciais sítios de fosforilação, a serina na posição 1177 (S1177) que está localizada na região próxima ao domínio redutase carboxi-terminal, parece ser um regulador crucial de sua atividade enzimática (Boo *et al.*, 2003). Diversas quinases e fosfatases participam na regulação da atividade da eNOS pela fosforilação e diferentes ativadores tem sido identificados e caracterizados na síntese de $NO^{\bullet}$. Estes últimos incluem estímulos mecânicos, fatores como o shear stress (Boo *et al*, 2002), fatores humorais como bradicinina (Harris *et al.,* 2002), fatores metabólicos como a insulina (Montagnani *et al*., 2001) e ativadores farmacológico, como a redução do colesterol HMG-CoA redutase (popularmente referidos como "estatinas").

A fosforilação do resíduo de S1177 resulta do aumento do fluxo de elétrons da enzima através do domínio redutase e reduz a sua associação à calmodulina. Como

resultado, eNOS torna-se mais ativa e produz mais NO, mesmo em níveis basais de cálcio citoplasmático (McCabe *et al.*, 2001). Existem várias linhas de evidências que indicam que a fosforilação da eNOS S1177 é crucial na disfunção vascular. Estudos tem demonstrado que o shear stress e o fluxo laminar aumentam a fosforilação da eNOS S1177 (Dimmeler *et al*., 1999; Gallis *et al.,* 1999) e modelos animais de estudo da hipercolesterolemia e aterosclerose, como camundongos *knockout* para apolipoproteina E (apoe), mostram diminuição da fosforilação da eNOS devido alterações no fluxo sangúineo laminar (Naoum *et al.,* 2004).

Após sua liberação no endotélio, o $NO^{\bullet}$ difunde-se para a célula muscular lisa vascular, promovendo vasodilatação. O alvo fisiológico do $NO^{\bullet}$ é a guanilato ciclase solúvel (Murad *et al.,* 1999; Napoli e Ignarro, 2001; Napoli *et al.,* 2006). O $NO^{\bullet}$ ativa a guanilato ciclase (GC) através de sua ligação à fração heme, resultando em um aumento nos níveis de guanosina mono-fosfato cíclica (GMPc). Na vasculatura, o GMPc exerce o relaxamento das células musculares lisas dependente de $NO^{\bullet}$. Esse efeito tem sido descrito como mediado pela fosforilação de proteínas, as quinases protéicas dependentes de GMPc, como a miosina de cadeia leve (Napoli e Ignarro, 2001; Napoli *et al.,* 2006). Atualmente, uma série de evidências indicam que $NO^{\bullet}$ também modula/regula uma série de ações através de mecanismos independentes do GMPc (Rabelink e Lusche, 2006; Liu e Huang, 2008), tais como sua ligação aos grupos sulfidril ligados às proteínas, para formar os compostos S-nitrosotióis (SNOs). Baseado em evidências experimentais, acredita-se que o $NO^{\bullet}$ e/ou espécies dele derivadas, podem nitrosar proteínas através de sua ligação a um metal de transição ou resíduo de cisteína de maneira reversível (Benhar *et al.*, 2008) por

meio do processo de S-nitrosação, o qual desempenha um papel central na transdução de sinal mediada pelo $NO^{\bullet}$. A S-nitrosação pode ser descrita como um sistema integral de sinalização, com reações de oxidação e redução de ampla distribuição em diversos tipos celulares, e didaticamente pode ser comparada com a sinalização exercida pela fosforilação protéica (Mannick e Schonhoff, 2002; Foster e McMahon, 2003). A grande maioria das proteínas contém resíduos de cisteína, porém, nem todos eles parecem ser passíveis de sofrerem S-nitrosação. Certos mecanismos conferem especificidade ao processo de S-nitrosação, o principal deles é o tipo de espécie gerada derivada do $NO^{\bullet}$. A reação do $NO^{\bullet}$ com o oxigênio gera diferentes óxidos, dependendo da concentração dos reagentes e do local onde ocorra. Esses óxidos de nitrogênio possuem afinidades variadas por metais de transição, tióis ou outros alvos, podendo, portanto, ligar-se a diversas proteínas e causar diferentes respostas celulares (Stamler *et al*., 1997). A compartimentalização da geração de $NO^{\bullet}$ e seus alvos num mesmo nível subcelular é outro mecanismo que confere especificidade à reação de S-nitrosação, uma vez que grande parte do $NO^{\bullet}$ produzido exerce seus efeitos num curto raio de ação (Mannick e Schonhoff, 2002). Contudo, a compartimentalização subcelular é um mecanismo necessário, porém não suficiente para conferir especificidade às reações de S-nitrosação. Foi descrita uma sequência de aminoácidos que facilita a ocorrência dessa reação, a qual foi descrita pela presença de um aminoácido básico (lisina, arginina ou histidina) e um aminoácido ácido (aspartato ou glutamato) ladeando ou na vizinhança próxima do resíduo de cisteína (Stamler *et al*., 1997). Então, apesar de ocorrer de forma não enzimática, a S-nitrosação é bastante específica, tendo como alvos resíduos de cisteína com características únicas. A nitrosação de tióis protéicos altera a forma e, portanto, a função da proteína alvo de maneira

reversível. A denitrosação ocorre de maneira não enzimática através de mudanças no pH, pO_2, equilíbrio redox, luz, entre outros fatores, que desestabilizam a ligação NO-tiol, levando à sua quebra (Stamler *et al.,* 2001*).* Essa reversibilidade da reação foi bem exemplificada nas reações de S-nitrosação que controlam a apoptose celular, onde caspase-3 S-nitrosada em células não estimuladas é denitrosada sobre ativação da via apoptótica Fas (Mannick *et al*., 1999) e também descrita na regulação da atividade da eNOS, a qual é constitutivamente S-nitrosada em células endoteliais em seu estado basal e quando estimulada por agonistas é denitrosada concomitantemente sua ativação (Erwin *et al*., 2005; Erwin e Mitchell, 2006).

Há concordância na literatura atual, de que a reduzida atividade biológica do $NO^{\bullet}$, causada tanto pela redução na síntese, descrita acima, como pelo aumento da degradação via estresse oxidativo. Sendo que este último tem sido identificado como o mecanismo de maior relevância no processo multifatorial da disfunção endotelial na participação das principais disfunções cardiovasculares (Pepine, 2009).

Dentre as espécies reativas de oxigênio (EROs) geradas pelas células do sistema cardiovascular, o superóxido ($O^{-\bullet}_2$) e o peróxido de hidrogênio (H_2O_2), são particularmente importantes na redução da biodisponibilidade do $NO^{\bullet}$. Nos sistemas biológicos, o superóxido tem uma meia vida curta devido à sua redução rápida em peróxido de hidrogênio pela enzima superóxido dismutase (SOD).

Aumentos nos níveis de $O^{-\bullet}_2$ podem ser advindos de inúmeras fontes como cadeia transportadora de elétrons das mitocôndrias, sistema NADPH oxidase, xantina oxidase, cicloxigenase e a própria eNOS que pode tornar-se desacoplada em condições de deficiência de substratos/ou co-fatores como o aumento dos níveis de dimetilarginina

assimétrica (ADMA) (De Gennaro *et al.*, 2009), oxidação aumentada de BH_4 (Loscalzo *et al.,* 1995; Sessa *et al.*, 2004; Li *et al.*, 2004; Li *et al.*, 2007;) elevadas concentrações de LDL (Pritchard e Groszek *et al.,* 1995) ou de glicose (Wever e Luscher, 1998; Tiefenbacher, 2001; Pou e Pou *et al*., 1992; Stroes *et al*., 1998; Vasquez-Vivar *et al*., 1998; Xia *et al*., 1998; Schmidt *et al.* 1992; Mayer *et al.*, 1995) (Madamanchi *et al*., 2005; Vendrov *et al.,* 2005). Assim, a principal fonte de H_2O_2 é a dismutação do $O^{-\bullet}_2$ a H_2O_2 através de reação espontânea ou catalisada pela SOD. Em presença de íons ferro (Fe^{2+}) ou outros metais de transição, o superóxido e o peróxido de hidrogênio são convertidos, via reação de Fenton, a radical hidroxil ($HO^{\bullet}$), que é responsável pela toxicidade celular associada às EROs.

A redução na biodisponibilidade de $NO^{\bullet}$ endotelial pode ocorrer via a inativação direta do $NO^{\bullet}$ por superóxido $O^{-\bullet}_2$, levando à formação do subproduto, o ânion peroxinitrito ($ONOO^-$). Essa é uma das principais e mais rápidas reações, que ocorre com uma constante de velocidade $10^{10}M^{-1}s^{-1}$, cinética favorável que faz com que a ocorrência seja limitada apenas pela capacidade de difusão dos gases no sitema biológico em questão (Fridovich, 1999; Quijano *et al*., 2005), assim o $O^{-\bullet}_2$ compete com a SOD pela parceria com o $NO^{\bullet}$.O $ONOO^-$ pode exercer vários efeitos nocivos nas células como oxidar lípides, sulfidril, BH_4, DNA e à nitração de resíduos de tirosina em várias proteínas (Ischiropoulos, 1998; Jourd'heuil *et al.,* 2001) chamado também de estresse nitrosativo. A nitração de tirosina pode levar à perda ou à modificação de função da mesma e parece representar um marcador potencial não específico da formação de $ONOO^-$ utilizado em estudos *in vivo* e considerada como um importante instrumento para estudo do estresse nitrosativo em

doenças humanas como envelhecimento (Ischiropoulos, 1998) e aterosclerose (Turko e Murad, 2002).

2- Hipertrofia cardíaca e Biodisponibilidade de $NO^{\bullet}$

A hipertofia ventricular esquerda (HVE) constitui um conjunto de alterações estruturais decorrentes do aumento das dimensões dos cardiomiócitos, da proliferação do tecido conjuntivo intersticial e da rarefação da microcirculação coronariana (Wollert e Drexler, 2002). Quanto às alterações funcionais, a hipertrofia causada, por exemplo, devido a sobrecargas hemodinâmicas, as quais podem conduzir à hipertrofia adaptada (fisiológica) ou mal-adaptada (patológica). A hipertrofia fisiológica é aquela desenvolvida em decorrência da sobrecarga hemodinâmica transitória, como as observadas no crescimento cardíaco durante a adolescência e a gestação, e em resposta a exercícios regulares. A hipertrofia patológica é aquela decorrente de sobrecarga hemodinâmica persistente (Kempf e Wollert, 2004). Nesta última foi verificado um aumento da produção de EROs no coração, a qual pode ser gerada devido ao aumento na concentração de Angiotensina-II (Ang-II) /NADPH oxidase (Lang *et al.*, 2000), hipercolesterolemia (Sato *et al.*, 2004), estresse mecânico no miocárdio (Aikawa *et al.*, 2001) e processos inflamatórios (Yao e Fukuda, 2006). O estresse oxidativo provocado pelo aumento de EROs foi correlacionada à hipertrofia ventricular esquerda em diversos modelos de estudo, como por exemplo, na hipertrofias induzidas por Ang II, fator de necrose tumoral-alfa (TNF-α) ou mesmo por meio da inibição do estresse mecânico por antioxidantes. Contudo, a fonte geradora de EROs e os seus alvos no coração hipertrofiado, ainda não se encontram

completamente elucidados, sendo que uma série estudos aponta a preponderância das NADPH oxidases vasculares (Nakagami *et al*, 2003).

O $NO^{\bullet}$ produzido no coração desempenha um papel anti-hipertrófico e é apontado como inibidor endógeno da cascata de sinalização que induz a hipertrofia cardíaca mal-adaptada. As primeiras evidências de que o $NO^{\bullet}$ pode apresentar efeitos anti-hipertróficos no coração foram obtidas em ratos tratados com L-name, onde o bloqueio da síntese de NO causou hipertrofia cardíaca por outro mecanismo que não hipertensão arterial (Numaguchi *et al*, 1995) e em ratos espontaneamente hipertensos (SHR), sob tratamento crônico com L-arginina (Matsuoka *et al.*, 1996). Posteriormente, tal papel do $NO^{\bullet}$ foi confirmado em camundongos que superexpressam óxido nítrico sintase endotelial (eNOS), nos quais o $NO^{\bullet}$ atenuou a hipertrofia cardíaca induzida pela infusão crônica de isoprenalina (ISO) (Ozaki *et al.*, 2002) indicando que o $NO^{\bullet}$ endógeno atua como modulador negativo para a hipertrofia cardíaca. E ainda por estudos em modelos de camundongos deficientes em nNOS ou eNOS, os quais desenvolveram hipertrofia cardíaca espontânea. Em linhas gerais, o aumento da atividade da eNOS nos cardiomiócitos e conseqüente aumento da concentração de $NO^{\bullet}$ promovem a diminuição da força de contração resultando em um efeito cardioprotetor mediado pelo GMPc, que se opõem ao efeito do estímulo excessivo pelas catecolaminas (Pelat *et al.*, 2005).

A origem e a concentração do $NO^{\bullet}$ desempenham um papel fundamental nos seus efeitos no remodelamento e na disfunção cardíaca. Baixas concentrações de $NO^{\bullet}$ produzidos pela eNOS exercem efeitos cardioprotetores. Por outro lado, grandes quantidades de $NO^{\bullet}$ como as concentrações produzidas pela iNOS exercem efeitos

prejudiciais e não são necessariamente cardioprotetores (Sam *et al.,* 2001; Zhang *et al*., 2007; Gilson *et al.,* 2007) o NO produzido pela iNOS possui ação citotóxica e citostática resultado de sua ação direta ou reação com outros compostos liberados durante o processo inflamatório. Isso pode, pelo menos em parte, explicar a formação de peroxinitrito aumentada, observada em cardiomiócitos de camundongos que superexpressam iNOS (Mungrue *et al*, 2002).

O $NO^{\bullet}$ em baixas concentrações produzido pelas NOS constitutivas protege os cardiomiócitos da injúria por isquemia/reperfusão via ativação da guanilil ciclase solúvel e formação do GMPc (Agullo *et al.,* 1999; Brunner *et al.,* 2003; Jones *et al.,* 1999; Jones *et al.,* 2004; Kanno *et al.,* 2000). Sobretudo, o $NO^{\bullet}$ demonstrou exercer efeitos benéficos no remodelamento do ventrículo esquerdo após infarto do miocárdio (Massion e Balligand, 2007). Os potenciais alvos para os efeitos mediados pelo $NO^{\bullet}$/GMPc nos cardiomiócitos incluem as fosfodiesterases reguladas pelo GMPc e a proteína quinase I dependente de GMPc (PKG I). Takimoto *et al*. (2005) demonstraram recentemente que a inibição da 5A-fosfodiesterase pode constitui uma ferramenta farmacológica para utilização dos efeitos benéficos do cGMP. Por meio da quebra de GMPc, pode ocorrer uma ativação sustentada da PKG, resultando na prevenção e reversão da hipertrofia cardíaca e do remodelamento, respectivamente (Takimoto *et al.,* 2005). A utilização de beta-bloqueadores com propriedades de incremento do $NO^{\bullet}$ (Sorrentino *et al*., 2006) e de outros doadores de $NO^{\bullet}$ (Fraccarollo *et al*., 2008) podem ser consideradas potenciais terapias neste âmbito.

Estudos prévios demonstraram o envolvimento da PKG I na regulação do estado inotrópico, no crescimento hipertrófico e na expressão gênica em cardiomiócitos expostos ao $NO^{\bullet}$ ou outros agentes que elevam GMPc (Feil *et al.,* 2003; Fielder *et al.,* 2002;

Heineke *et al.,* 2003; Wegener *et al.,* 2002; Wollert *et al.,* 2002b). Recentemente, foi demonstrado que a PKG I protege os cardiomiócitos da morte celular por apoptose durante a injúria por isquemia/reperfusão, em parte, via inibição da sinalização TAB1-p38 (Fielder *et al*., 2006). Assim, o $NO^{\bullet}$ apresenta um efeito pró-apoptótico concentração-dependente em cardiomiócitos. Em baixas concentrações (250uM) o doador de $NO^{\bullet}$ S-nitroso-N-acetilpenicilamina (SNAP) inibe a hipertrofia do cardiomiócito, enquanto que concentrações de 1000 uM deste são requeridas para provocar a ativação de caspases, fragmentação de DNA e apoptose (Wollert *et al.,* 2002). Estudos de Feng (2002) em camundongos eNOS-/- demonstraram que a apoptose de cardiomiócitos foi significativamente aumentada no miocárdio durante o desenvolvimento fetal e neonatal, indicando que a produção de óxido nítrico basal via eNOS protege cardiomiócitos da apoptose.

3- Aterogênese e Biodisponibilidade de $NO^{\bullet}$

A hipercolesterolemia e outras doenças lipidêmicas que levam à aterosclerose têm sido associadas à redução na biodisponibilidade de $NO^{\bullet}$ devido ao aumento de estresse oxidativo, prejuízo na taxa de "turnover" da eNOS além de um aumento da presença de ADMA (Vanhoutte *et al.,* 2009). Em animais e humanos, a hipercolesterolemia reduz a dilatação/relaxamento dependente do endotélio (Jain e Ridker, 2005; Michel e Vanhoutte 2010) e o ínicio do processo de aterogênese pode ser percebido após apenas uma semana de exposição à dieta hipercolesterolêmica, com monócitos aderidos à superfície endotelial e, subsequentemente, atingindo a íntima vascular a aderência dos monócitos ao endotélio pode ser reduzida pelo estímulo à maior produção de $NO^{\bullet}$. (Tsao *et al.,* 1994). Assim, a manutenção da biodisponibilidade de $NO^{\bullet}$ adequada no ambiente vascular condições que

inibem o desenvolvimento do ateroma, uma vez que irá promover a inibição de: (Chanon *et al.,* 2000)

1. Adesão, agregação e ativação das plaquetas induzida pela trombina;
2. Proliferação, migração de células da musculatura lisa e síntese de matriz extracelular;
3. Adesão e ativação de neutrófilos e monócitos, apresentando efeitos inflamatórios;
4. Formação de LDL oxidada que é altamente aterogênica, apresentando efeitos antioxidantes.

A aterosclerose constitui uma doença com desenvolvimento dinâmico e presença de elementos característicos nas diferentes fases do processo. Contudo, marcadores específicos de uma determinada fase e sua correlação com as alterações estruturais decorrentes da doença, ainda encontram-se em estudo. Os diferentes estágios são caracterizados por meio de evidências estruturais e da expressão de fatores indicadores ou marcadores nas lesões, segundo Lusis *et al* (2004). Neste contexto, tem sido verificado o papel do receptor CD40 e seu ligante CD40L em vários estágios da aterosclerose, compreendendo fases de: início, evolução e complicações agudas após a ruptura da placa. Uma série de estudos mostraram esta interação por meio de sua expressão em uma ampla variedade de células e foi demonstrado em artérias carótida e aorta de humanos, a presença de CD40-CD40L em sítios de inflamação crônica, incluindo lesões ateroscleróticas (Reul *et al.*, 1997; Mach *et al.*, 1997; Gaweco *et al.*, 1999; Afford *et al.*, 1999).

Foi demonstrado que a ligação entre CD40 e CD40L induz a expressão de moléculas de adesão em células endoteliais (Karmann *et al.*, 1995; Hollenbaugh *et al.*, 1995; Yellin *et al.*, 1995) e estimula a liberação de quimiocinas, como IL-8 e MIP-1-α

(proteína inflamatória de macrófago 1α) (Kiener *et al.*, 1995; Henn *et al.*, 1998; Kornbluth *et al.*, 1998), e que tais moléculas participam localmente nas fases iniciais da aterosclerose. Camundongos LDLr-/- (*knockout* para o receptor de LDL) tratados com anti-corpos contra CD40L e sob dieta hipercolesterolêmica por 12 semanas demonstraram grande redução na formação de lesões ateroscleróticas (Mach *et al.*, 1998).

4- Camundongos LDLr-/-

Camundongos *knockout* para o receptor LDL (Low Density Lipoprotein) desenvolvem lesões avançadas em resposta a uma dieta rica em gordura e constitui-se de um dos modelos mais utilizados para estudos genéticos e fisiológicos do processo aterosclerótico (Tamgirala *et al.,* 1995). Uma série de estudos mostra que lesões iniciais foram observadas na parede arterial em animais alimentados com dieta hiperlipidêmica em curto espaço de tempo (10-15 dias) e se constituem do acúmulo de partículas de lipoproteína e agregados na camada íntima, locais de predileção para a formação de lesão (Paigen *et al.,* 1987).

Estudos prévios de nosso laboratório mostraram que camundongos machos LDLr-/- apresentam fenótipo hipertenso em relação ao seu *background* (C57Bl6) e que após serem submetidos à dieta hiperlipidêmica durante 15 dias, esses animais não apresentaram incrementos nos valores da pressão arterial, contudo, desenvolvem outras diversas alterações cardiovasculares como formação da placa aterosclerótica (Krieger *et al*., 2006); arritmia (Caceres *et al.*, 2010) e desenvolvimento de hipertrofia ventricular esquerda, a qual foi caracterizada pelos aumentos no indíce ventricular esquerdo relativo (peso ventrículo mg/peso animal g), na dimensão dos cardiomiócitos, e na deposição de colágeno intersticial e perivascular (Garcia *et al.*, 2008). Nesses últimos anos, nosso laboratório tem

estudado compostos potenciais doadores de $NO^{\bullet}$, bem como os S-nitrosotióis (RSNO) e sua aplicação em doenças cardiovasculares. O tratamento com o composto doador de $NO^{\bullet}$ denominado S-nitroso-N-acetilcisteína (SNAC) demonstrou exercer efeito vasodilatador mais prolongado do que o nitroprussiato de sódio em ratos SHR, agindo através de mecanismos dependentes e independentes de GMPc (Ricardo *et al*., 2002). Nossos estudos em camundongos LDLr-/- tratados com a SNAC demonstraram resultados e mecanismos promissores nas seguintes alterações cardiovasculares associadas à dislipidemia: i) 55% de impedimento na formação da placa de aterosclerose em camundongos LDLr-/- sob dieta hiperlipidêmica por 15 dias via redução do estresse oxidativo (Santos *et al.*, 2005); ii) modulação da função cardíaca por meio do aumento do acoplamento do receptor β_2-adrenérgico à proteína G inibitória (Gi), o que resultou na proteção contra arritmia cardíaca (Caceres *et al.*, 2010) iii) 100% de eficácia no bloqueio do desenvolvimento da hipertrofia ventricular esquerda via antiinflamatória, pois associada ao desenvolvimento da placa foi verificada a presença de hipertrofia ventricular esquerda nestes camundongos tratados com dieta hiperlipideêmica (Garcia *et al.*, 2008); dados mostrados na tabela 1.

TABELA 1. Valores laboratório em camundongos W. C. H. e H+S. (Traduzido de Garcia *et al*.. 2008)

Grupo	W (n = 6)	C (n = 6)	H (n = 6)	H+S (n = 6)
PAS (mm Hg)	127 ± 2.3	140 ± 2.7*	142 ± 1.9*	145 ± 1.8*
FC (bpm)	579 ± 9.9	520 ± 8.1*	516 ± 9.1*	517 ± 11.1*
Total PVE (mg)	85.8 ± 2.0	84.6 ± 1.7	96.4 ± 2.9†	80.1 ± 5.0†
Total PC (g)	27,9 ± 0,4	25,4 ± 0,8*	23,1 ± 0,5*†	23,7 ± 0,7*†
PVE/PC (mg/g)	3.08 ± 0.04	3.34 ± 0.07	4.17 ± 0.09†	3.38 ± 0.23‡
Diâmetro Cardiomiócito (µm)	18 ± 0.5	19 ± 0.7	25 ± 0.6†	20 ± 0.7‡
Área colágeno intersticial (%)	2.8 ± 0.3	3.1 ± 0.10	8.6 ± 0.47†	2.9 ± 0.32‡
Área colágeno perivascular (%)	1.3 ± 0.1	1.6 ± 0.1	2.0 ± 0.05†	1.5 ± 0.07‡

Dados expressos média ± EPM.
PAS, pressão arterial sistólica; FC, frequência cardíaca; PVE, peso ventricular esquerdo; PC, peso corporal; PVE/PC razão peso ventricular esquerdo/peso corporal; W, camundongos C57Bl6; C, camundongos LDLr-/- alimentados com dieta comercial; H, camundongos LDLr-/- alimentados com dieta aterogênica; H + S, camundongos LDLr-/- alimentados com dieta aterogênica e tratados com SNAC.
PAS e FC não foram significativamente diferentes entre camundongos C, H e H + S.
*$P < 0,05$ comparados aos camundongos W.
†$P < 0,05$ comparados aos camundongos C (ANOVA + Teste Tukey).
‡$P < 0,05$ comparados ao camundongos H.

II – OBJETIVOS

Objetivo Geral:

Avaliar a biodisponibilidade de $NO^{\bullet}$ em função das alterações cardiovasculares, especificamente na hipertrofia ventricular esquerda e aterosclerose, por meio da caracterização das suas vias de síntese/degradação e identificação de seus possíveis alvos.

Objetivos Específicos:

1. Avaliar o papel protetor do doador de $NO^{\bullet}$ S-nitroso-N-acetilcisteína no remodelamento cardíaco em camundongos LDLr-/- por meio de sua ação no estresse oxidativo/nitrosativo, expressão e S-nitrosação do betadrenoceptor-2 e na apoptose;

2. Avaliar a biodisponibilidade de $NO^{\bullet}$ na fase inicial da aterogênese em camundongos LDLr-/- no curso temporal de 15 a 60 dias, por meio da quantificação de parâmetros sistêmicos representados pela pressão arterial, perfil lipidêmico e ateroma e de parâmetros locais representados pela atividade e expressão da via NO/NOS e suas modificações pós-traducionais no processo inflamatório via CD40-CD40L.

III - REFERÊNCIAS BIBLIOGRÁFICAS

Afford SC, Randhawa S, Eliopoulos AG, Hubscher SG, Yong LS, Adams DH. CD40 activation induces apoptosis in cultured human hepatocytes via induction of cell surface fas ligand expression and amplifies fas-mediated hepatocyte death during allograft rejection. **J Exp Med** 189:441-46, 1999.

Agulló L, García-Dorado D, Inserte J, Paniagua A, Pyrhonen P, Llevadot J, Soler-Soler J. L-arginine limits myocardial cell death secondary to hypoxiareoxygenation by a cGMP-dependent mechanism. **Am J Physiol Heart Circ Physiol** 276:H1574–H1580, 1999.

Aikawa R, Nagai T, Tanaka M, Zou Y, Ishihara T, Takano H, Hasegawa H, Akazawa H, Mizukami M, Nagai R, Komuro I. Reactive oxygen species in mechanical stress-induced cardiac hypertrophy. **Biochem Biophys Res Commun** 289:901-7, 2001.

Alderton WK, Cooper CE, Knowles RG. Nitric oxide synthases: structure, function and inhibition. **Biochem J** 357:593-615, 2001.

Andrew PJ, Mayer B. Enzymatic function of nitric oxide synthases. **Cardiovasc Res** 43(3):521-31, 1999.

Arstall MA, Sawyer DB, Fukazawa R, Kelly RA. Cytokine-mediated apoptosis in cardiac myocytes: the role of inducible nitric oxide synthase induction and peroxynitrite generation. **Circ Res** 85:829-40, 1999.

Gallis B, Corthals GL, Goodlett DR, Ueba H, Kim F, Presnell SR, Figeys D, Harrison DG, Berk BC, Aebersold R, Corson MA. Identification of flow-dependent endothelial nitric-oxide synthase phosphorylation sites by mass spectrometry and regulation of phosphorylation and nitric oxide production by the phosphatidylinositol 3-kinase inhibitor Ly294002. **J Biol Chem**. 274:30101–30108, 1999.

Balligand JL, Kobzik L, Han X, Kaye DM, Belhassen L, O'Hara DS, Kelly RA, Smith TW, Michel T.Nitric oxide-dependent parasympathetic signaling is due to activation of constitutive endothelial (type III) nitric oxide synthase in cardiac myocytes. **J Biol Chem** 270:14582-6, 1995.

Benhar M, Forrester MT, Hess DT, Stamler JS. Regulated protein denitrosylation by cytosolic and mitochondrial thioredoxins. **Science** 320(5879):1050-4, 2008.

Boo YC, Kim HJ, Song H, Fulton D, Sessa W. Coordinated regulation of endothelial nitric oxide synthase activity by phosphorylation and subcellular localization. **Free Radic Biol Med** 41(1):144-53, 2006.

Boo YC, Sorescu G, Boyd N, Shiojima I, Walsh K, Du J, Jo H. Shear stress stimulates phosphorylation of endothelial nitric-oxide synthase at Ser1179 by Akt-independent mechanisms: role of protein kinase A. **J Biol Chem** 277(5):3388–3396, 2002.

Boo YC. and Jo H, Flow-dependent regulation of endothelial nitric oxide synthase: role of protein kinases. **Am J Physiol Cell Physiol** 285:C499–C508, 2003.

Brunner F, Maier R, Andrew P, Wolkart G, Zechner R, Mayer B. Attenuation of myocardial ischemia/reperfusion injury in mice with myocytespecific overexpression of endothelial nitric oxide synthase. **Cardiovasc Res** 57:55–62, 2003.

Caceres VM, Moura AL, Wanschel AC BA, Krieger, MH, Spadari, RC. Coupling of beta-2 adrenoceptors to inhibitory G protein in atria of hypercholesterolemic LDLr-/- mice. *Britsh Journal. (submitted).*

Cai H. NAD(P)H oxidase-dependent self-propagation of hydrogen peroxide and vascular disease. **Circ Res** 96:818–822, 2005.

Channon KM, Qian H, George SE. Nitric oxide in atherosclerosis and vascular injury. **Arterioscler Throm Vasc Biol** 20:1873-1881, 2000.

Dudzinski DM, Igarashi J, Greif D, Michel T. The regulation and pharmacology of endothelial nitric oxide synthase. **Annu Rev Pharmacol Toxicol** 46:235–276, 2006.

De Gennaro Colonna V, Bianchi M, Pascale V, Ferrario P, Morelli F, Pascale W, Tomasoni L, Turiel M. Asymmetric dimethylarginine (ADMA): an endogenous inhibitor of nitric oxide synthase and a novel cardiovascular risk molecule. **Med Sci Monit** 15(4):RA91-101, 2009.

Erwin PA, Lin AJ, Golan DE, Michel, T. **J Biol Chem** 280:19888–19894, 2005.

Erwin PA, Mitchell DA, Sartoretto J, Marletta MA, Michel T. Subcellular targeting and differential S-nitrosylation of endothelial nitric-oxide synthase. **J Biol Chem** 281(1):151–157, 2006.

Feil R, Lohmann SM, de Jonge H, Walter U, Hofmann F. Cyclic GMP-dependent protein kinases and the cardiovascular system: insights from genetically modified mice. **Circ Res** 93:907–916, 2003.

Fiedler B, Feil R, Hofmann F, Willenbockel C, Drexler H, Smolenski A, Lohmann SM, Wollert KC. cGMP-dependent protein kinase type I inhibits TAB1-p38 mitogen-activated protein kinase apoptosis signaling in cardiac myocytes. **J Biol Chem** 281:32831–32840, 2006.

Fiedler B, Lohmann SM, Smolenski A, Linnemuller S, Pieske B, Schroder F, Molkentin JD, Drexler H, Wollert KC.Inhibition of calcineurin-NFAT hypertrophy signaling by cGMP-dependent protein kinase type I in cardiac myocytes. **Proc Natl Acad Sci USA** 99:11363–11368, 2002.

Foster MW, McMahon TJ, Stamler JS. "S-nitrosylation in health and disease." **Trends Mol Med** 9(4): 160-8, 2003.

Fraccarollo D, Widder JD, Galuppo P, Thum T, Tsikas D, Hoffmann M, Ruetten H, Ertl G, Bauersachs J. Improvement in left ventricular remodeling by the endothelial nitric oxide synthase enhancer AVE9488 after experimental myocardial infarction. **Circulation** 118:818–827, 2008.

Fridovich I, Fundamental aspects of reactive oxygen species, or what's the matter with oxygen? **Ann N Y Acad Sci** 893:13-18, 1999.

Fulton D, Gratton JP, McCabe TJ, Fontana J, Fujio Y, Walsh K, Franke TF, Papapetropoulos A, Sessa WC. Regulation of endothelium-derived nitric oxide production by the protein kinase Akt. **Nature** 399:597-601, 1999.

Furchgott RF, Zawadzki JV. The obligatory role of endothelial cells in the relaxation of arterial smooth muscle by acetylcholine. **Nature** 288:373-6, 1980.

Garcia JA, dos Santos L, Moura AL, Ricardo KF, Wanschel AC, Shishido SM, Spadari-Bratfisch RC, de Souza HP, Krieger MH. S-nitroso-N-acetylcysteine (SNAC) prevents myocardial alterations in hypercholesterolemic LDL receptor knockout mice by anti-inflammatory action. **J Cardiovasc Pharmacol** 51:78-85, 2008.

Gaweco AS, Wiesner RH, Yong S, Krom R, Porayko M, Chejfec G, McClatchey KD, Van Thiel DH. CD40L (CD154) expression in human liver allografts during chronic ductopenic rejection. **Live Transpl Surg** 5:1-7, 1999.

Gilson WD, Epstein FH, Yang Z, Xu Y, Prasad KM, Toufektsian MC, Laubach VE, French BA. Borderzone contractile dysfunction is transiently attenuated and left ventricular structural remodeling is markedly reduced following reperfused

myocardial infarction in inducible nitric oxide synthase knockout mice. **J Am Coll Cardiol** 50:1799–1807, 2007.

Guo H, Shi Y, Liu L, Sun A, Xu F, Chi J. Rosuvastatin inhibits MMP-2 expression and limits the progression of atherosclerosis in LDLR-deficient mice. **Arch Med Res** 40(5):345-51, 2009.

Razavi HM, Hamilton JA, Feng Q. Modulation of apoptosis by nitric oxide: implications in myocardial ischemia and heart failure. **Pharmacology & Therapeutics** 106:147–162, 2005.

Heineke J, Kempf T, Kraft T, Hilfiker A, Morawietz H, Scheubel RJ, Caroni P, Lohmann SM, Drexler H, Wollert KC. Downregulation of cytoskeletal muscle LIM protein by nitric oxide: impact on cardiac myocyte hypertrophy. **Circulation** 107:1424–1432, 2003.

Henn V, Slupsky JR, Grafe M, Anagnostopoulos I, Forster R, Muller-Berghaus G, Kroczek RA . CD40 ligand on activated platelets triggers an inflammatory reaction of endothelial cells. **Nature** 391:591-94, 1998.

Hollenbaugh D, Grosmaire LS, Kullas CD, Chalupny NJ, Braesch-Andersen S, Noelle RJ, Stamenkovic I, Ledbetter JA, Aruffo A. The human T cell antigen gp39, a member of the TNF gene family, is a ligand for the CD40 receptor: expression of a soluble form of gp39 with B cell co-stimulatory activity. **Embo J** 11:4313-21, 1992.

Ing DJ, Zang J, Dzau VJ, Webster KA, Bishopric NH. Modulation of cytokineinduced cardiac myocyte apoptosis by nitric oxide, Bak, and Bcl-x. **Circ Res** 84:21-33, 1999.

Ischiropoulos H. Biological tyrosine nitration: a pathophysiological function of nitric oxide and reactive oxygen species. **Arch Biochem Biophys** 356:1-11, 1998.

Jourd'heuil D, Jourd'heuil FL, Kutchukian PS, Musah RA, Wink DA, Grisham MB. Reaction of superoxide and nitric oxide with peroxynitrite. Implications for peroxynitrite-mediated oxidation reactions in vivo. **J Biol Chem** 276(31):28799-805, 2001.

Naoum JJ, Zhang S, Woodside KJ, Song W, Guo Q, Belalcazar LM, Hunter GC. Aortic eNOS expression and phosphorylation in APO-E knockout mice: differing effects of rapamycin and simvastatin. **Surgery** 136:323–328, 2004.

Jain MK, Ridker PM. Anti-inflammatory effects of statins: clinical evidence and basic mechanisms. **Nat Rev Drug Discov** 4(12):977–987, 2005.

Jones SP, Girod WG, Palazzo AJ, Granger DN, Grisham MB, Jourd'Heuil D, Huang PL, Lefer DJ. Myocardial ischemia-reperfusion injury is exacerbated in absence of endothelial cell nitric oxide synthase. **Am J Physiol Heart Circ Physiol** 276:H1567–H1573, 1999.

Jones SP, Greer JJ, Kakkar AK, Ware PD, Turnage RH, Hicks M, van Haperen R, de Crom R, Kawashima S, Yokoyama M, Lefer DJ.Endothelial nitric oxide synthase overexpression attenuates myocardial reperfusion injury. **Am J Physiol Heart Circ Physiol;** 286:H276–H282, 2004.

Kanno S, Lee PC, Zhang Y, Ho C, Griffith BP, Shears LL 2nd, Billiar TR. Attenuation of myocardial ischemia/reperfusion injury by superinduction of inducible nitric oxide synthase. **Circulation** 101:2742–2748, 2000.

Karmann K, Hughes CC, Scheeechner J, Fanslow WC, Pober JS. CD40 on human endothelial cells: inducibility by cytokines and functional regulation of adhesion molecule expression. **Proc Natl Acad Sci** 92:4342-6, 1995.

Kempf T, Wollert KC. Nitric oxide and the enigma of cardiac hypertrophy. **Bioessays** 6:608-15, 2004.

Kiener PA, Moran-Davis P, Rankin BM, Wahl AF, Aruffo A, Hollenbaugh D. Stimulation of CD40 with purified soluble gp39 induces proinflammatory responses in human monocytes. **J Exp Med** 155:4917-25, 1995.

Klimaschewski L, Kummer W, Mayer B, Couraud JY, Preissler U, Philippin B, Heym C. Nitric oxide synthase in cardiac nerve fibers and neurons of rat and guinea pig heart. **Circ Res** 71:1533-7, 1992.

Kojda G, Harrison D. Interactions between NO and reactive oxygen species: pathophysiological importance in atherosclerosis, hypertension, diabetes and heart failure. **Cardiovasc Res** 43:562-71, 1999.

Kornbluth RS, Kee K, Richman DD. CD40 ligand (CD154) stimulation of macrophages to produce HIV-1-suppressive beta-chemokines. **Proc Natl Acad Sci** 95:5205-10, 1998.

Krieger, J E. Bases Moleculares das Doenças Cardiovasculares. 1ed. São Paulo: Atheneu; 2008. p415.

Krieger MH, Santos KF, Shishido SM, Wanschel AC, Estrela HF, Santos L, De Oliveira MG, Franchini KG, Spadari-Bratfisch RC, Laurindo FR. Antiatherogenic effects of S-nitroso-N-acetylcysteine in hypercholesterolemic LDL receptor knockout mice. **Nitric Oxide** 14:12-20, 2006.

Lang D, Mosfer SI, Shakesby A, Donaldson F, Lewis MJ. Coronary microvascular endothelial cell redox state in left ventricular hypertrophy: the role of angiotensin II. **Circ Res** 86:463-9, 2000.

Lerman A, Burnett Jr. JC. Intact and altered endothelium in regulation of vasomotion. **Circulation** 86(6):III12-9, 1992.

Li JM, Shah AM. Endothelial cell superoxide generation: regulation and relevance for cardiovascular pathophysiology. **Am J Physiol Regul Integr Comp Physiol** 287(5):R1014–R1030, 2004.

Li PL, Gulbins E. Lipid rafts and redox signaling. **Antioxid Redox Signal** 9(9):1411–1415, 2007.

Libby P, Ridker PM, Maseri A. Inflammation and atherosclerosis. **Circulation** 105:1135–1143, 2002.

Libby P, Theroux P. Pathophysiology of coronary artery disease. **Circulation** 111(25):3481-8, 2005.

Libby P. Inflammation in atherosclerosis. Nature. 2002;420:868–874. Liu, V. W. T. and Huang, P. L., Cardiovascular roles of nitric oxide: A review of insights from nitric oxide synthase gene disrupted mice. **Cardiovasc Res** 77:19- 29, 2008.

Loscalzo J, Welch G Nitric oxide and its role in the cardiovascular system. **Prog Cardiovasc Dis** 38(2):87–104, 1995.

Lusis AJ, Mar R, Pajukanta P. Genetics of atherosclerosis. **Annu Rev Genomics Hum Genet** 5:189-218, 2004.

Harris MB, Ju H, Venema VJ, Liang H, Zou R, Michell BJ, Chen ZP, Kemp BE, Venema RC. Reciprocal phosphorylation and regulation of endothelial nitric-oxide

synthase in response to bradykinin stimulation. **J Biol Chem** 276 (19)16587–16591, 2001.

Mach F, Schonbeck U, Sukhova GK, Atkinson E, Libby P. Reduction of atherosclerosis in mice by inhibition of CD40 signalling. **Nature** 394:200-3, 1998.

Mach F, Schonbeck U, Sukhova GK, Bourcier T, Bonnefoy JY, Pober JS, Libby P. Functional CD40 ligand is expressed on human vascular endothelial cells, smooth muscle cells, and macrophages: implications for CD40-CD40 ligand signaling in atherosclerosis. **Proc Natl Acad Sci** 94:1931-36, 1997.

Madamanchi NR, Vendrov A, Runge MS. Oxidative stress and vascular disease. **Arterioscler Thromb Vasc Biol** 25:29–38, 2005.

Mannick JB, Hausladen A, Liu L, Hess DT, Zeng M, Miao QX, Kane LS, Gow AJ, Stamler JS. Fas-induced caspase denitrosylation. **Science** 284(5414):651-4, 1999.

Mannick JB, Schonhoff CM. "Nitrosylation: the next phosphorylation?" **Arch Biochem Biophys** 408(1):1-6, 2002.

Massion PB, Balligand JL. Relevance of nitric oxide for myocardial remodeling. **Curr Heart Fail Rep** 4:18–25, 2007.

Matsuoka H, Nakata M, Kohno K, Koga Y, Nomura G, Toshima H, Imaizumi T. Chronic L-arginine administration attenuates cardiac hypertrophy in spontaneously hypertensive rats. **Hypertension** 27:14-8, 1996.

Mayer B, Werner ER. In search of a function for tetrahydrobiopterin in the biosynthesis of nitric oxide. **Naunyn Schmiedebergs Arch Pharmacol** 351:453-63, 1995.

Michel T, Vanhoutte PM. Cellular signaling and NO production. **Pflugers Arch** 1432-2013, 2010.

Moncada S, Palmer RM, Higgs EA. The biological significance of nitric oxide formation from L-arginine. **Biochem Soc Trans** 17:642-4, 1989.

Montagnani M, Chen H, Barr VA Quon MJ, Insulin-stimulated activation of eNOS is independent of Ca2+ but requires phosphorylation by Akt at Ser1179. **J Biol Chem** 276(32):30392–30398, 2001.

Morgan HE, Gordon EE, Kira Y, Chua HL, Russo LA, Peterson CJ, McDermott PJ, Watson PA. Biochemical mechanisms of cardiac hypertrophy. **Ann Rev Physiol** 49:533-43, 1987.

Mungrue IN, Gros R, You X, Pirani A, Azad A, Csont T, Schulz R, Butany J, Stewart DJ, Husain M. Cardiomyocyte overexpression of iNOS in mice results in peroxynitrite generation, heart block, and sudden death. **J Clin Invest** 109:735–743, 2002.

Murad F. "Cellular signaling with nitric oxide and cyclic GMP." **Braz J Med Biol Res** 32(11):1317-27, 1999.

Nakagami H, Takemoto M, Liao JK. NADPH oxidase-derived superoxide anion mediates angiotensin II-induced cardiac hypertrophy. **J Mol Cell Cardiol** 7:851-859, 2003.

Napoli C, de Nigris F, Williams-Ignarro S, Pignalosa O, Sica V, Ignarro LJ, Nitric oxide and atherosclerosis: An update. **Nitric Oxide** 15:265-279, 2006.

Napoli C, Ignarro L J, Nitric oxide and atherosclerosis. **Nitric Oxide** 5:88-97, 2001.

Numaguchi K, Egashira K, Takemoto M, Kadokami T, Shimokawa H, Sueishi K, Takeshita A. Chronic inhibition of nitric oxide synthesis cause coronary microvascularremodeling in rats. **Hypertension** 26: 957-62, 1995.

Ozaki M, Kawashima S, Yamashita T, Hirase T, Ohashi Y, Inoue N, Hirata K, Yokoyama M. Overexpression of endothelial nitric oxide synthase attenuates cardiac hypertrophy induced by chronic isoproterenol infusion. **Circ J** 66:851-6, 2002.

Paigen B, Morrow A, Holmes PA, Mitchell D, Williams RA. Quantitative assessment of atherosclerotic lesions in mice. **Atherosclerosis**. 68(3):231-40, 1987.

Palmer RM, Ferrige AG, Moncada S. Nitric oxide release accounts for the biological activity of endothelium-derived relaxing factor. **Nature** 327:524-6, 1987.

Pelat M, Massion PB, Balligand JL. Nitric oxide "at heart": emerging paradigms after a decade. **Arch Mal Coeur Vaiss** 98(3):242-8, 2005.

Pepine CJ The impact of nitric oxide in cardiovascular medicine: untapped potential utility. **Am J Med** 122:S10-5, 2009.

Pou S, Pou WS, Bredt DS, Snyder SH, Rosen GM.Generation of superoxide by purified brain nitric oxide synthase. **J Biol Chem**, 267:24173-6. 1992.

Pritchard KA Jr, Groszek L, Smalley DM, Sessa WC, Wu M, Villalon P, Wolin MS, Stemerman MB. Native low-density lipoprotein increases endothelial cell nitric oxide synthase generation of superoxide anion. **Circ Res**, 77:510-8.1995.

Quijano C, Romero N, Radi R. Tyrosine nitration by superoxide and nitric oxide fluxes in biological systems: modeling the impact of superoxide dismutase and nitric oxide diffusion. **Free Radic Biol Med** 39:728-41. 2005.

Rabelink, TJ. and Luscher, TF., Endothelial Nitric Oxide Synthase: Host defense enzyme of the endothelium? **Arterioscler Thromb Vasc Biol** 26:267-271, 2006.

Reul RM, Fang JC, Denton MD, Geehan C, Long C, Mitchell RN, Ganz P, Briscoe DM. CD40 and CD40 ligand (CD154) are coexpressed on microvessels in vivo in human cardiac allograft rejection. **Transplantetion** 64:1765-74, 1997.

Ricardo KF, Shishido SM, de Oliveira MG, Krieger MH. Characterization of the hypotensive effect of S-nitroso-N-acetylcysteine in normotensive and hypertensive conscious rats. **Nitric Oxide** 7(1):57-66, 2002.

Rubbo H, Radi R, Anselmi D, Kirk M, Barnes S, Butler J, Eiserich JP, Freeman BA. Nitric oxide reaction with lipid peroxyl radicals spares alphatocopherol during lipid peroxidation. Greater oxidant protection from the pair nitric oxide/alpha-tocopherol than alpha-tocopherol/ascorbate. **J Biol Chem**, 275:10812-8, 2000.

Dimmeler S, Fleming I, Fisslthaler B, Hermann C, Busse R, Zeiher AM.Activation of nitric oxide synthase in endothelial cells by Akt-dependent phosphorylation. **Nature** 399:601–605, 1999.

Sam F, Sawyer DB, Xie Z, Chang DL, Ngoy S, Brenner DA, Siwik DA, Singh K, Apstein CS, Colucci WS. Mice lacking inducible nitric oxide synthase have improved left ventricular contractile function and reduced apoptotic cell death late after myocardial infarction. **Circ Res** 89:351–356, 2001.

Sato K, Komaru T, Shioiri H, Takeda S, Takahashi K, Kanatsuka H, Nakayama M, Shirato K.Hypercholesterolemia impairs transduction of vasodilator signals derived from ischemic myocardium: myocardium-microvessel cross-talk. **Arterioscler Thromb Vasc Biol** 24 (11):2034-9, 2004.

Schmidt K, Werner ER, Mayer B, Wachter H, Kukovetz WR. Tetrahydrobiopterin-dependent formation of endotheliumderived relaxing factor (nitric oxide) in aortic endothelial cells. **Biochem J** 281:297-300, 1992.

Schulz R, Smith JA, Lewis MJ, Moncada S. Nitric oxide synthase in cultured endocardial cells of the pig. **Br J Pharmacol** 104:21-4, 1991.

Sessa WC. eNOS at a glance. **J Cell Sci** 117:2427-9, 2004.

Shaul PW, Anderson RG. Role of plasmalemmal caveolae in signal transduction. **Am J Physiol** 275:L843-51, 1998.

Sorrentino SA, Doerries C, Mohmand W, Akbar R, Besler C, Schaefer A et al. Effect of nebivolol vs. metoprolol on endothelial function, endothelial progenitor cell mobilization and left ventricular remodeling and dysfunction early after myocardial infarction. **Circulation** 114:370, 2006. (abstract).

Stamler JS, Toone EJ, Lipton SA, Sucher NJ."(S)NO signals: translocation, regulation, and a consensus motif." **Neuron** 18(5):691-6, 1997.

Stamler JS, Lamas S, Fang FC."Nitrosylation. the prototypic redox-based signaling mechanism." **Cell** 106(6):675-83, 2001.

Stroes E, Hijmering M, van Zandvoort M, Wever R, Rabelink TJ, van Faassen EE. Origin of superoxide production by endothelial nitric oxide synthase. **FEBS Lett**, 438:161-4, 1998.

Sussman A, Mcculloch A, Borg TK. Dance band on the titanic: biomechanical signaling in cardiac hypertrophy. **Circ Res** 91:888-98, 2002.

McCabe TJ, Fulton D, Roman LJ, Sessa WC. Enhanced electron flux and reduced calmodulin dissociation may explain 'calcium-independent' eNOS activation by phosphorylation. **J Biol Chem**. 275:6123–6128, 2000.

Takimoto E, Champion HC, Li M, Belardi D, Ren S, Rodriguez ER, Bedja D, Gabrielson KL, Wang Y, Kass DA. Chronic inhibition of cyclic GMP phosphodiesterase 5A prevents and reverses cardiac hypertrophy. **Nat Med** 11:214–222, 2005.

Tambascia RC, Fonseca PM, Corat PDC, Moreno H, Saad MJA, Franchini KG. Expression and distribution of NOS1 and NOS3 in the myocardium of angiotensin II infused rats. **Hypertension** 37:1423-8, 2000.

Tangirala RK, Rubin EM, Palinski W. Quantitation of atherosclerosis in murine models: correlation between lesions in the aortic origin and in the entire aorta, and differences in the extent of lesions between sexes in LDL receptor-deficient and apolipoprotein E-deficient mice. **J Lipid Res** 36(11):2320-8, 1995.

Tiefenbacher, C. P. Tetrahydrobiopterin: a critical cofactor for eNOS and a strategy in the treatment of endothelial dysfunction? **Am J Physiol Heart Circ Physiol** 280:H2484-8, 2001.

Tsao PS, McEvoy LM, Drexler H, Butcher EC, Cooke JP. Enhanced endothelial adhesiveness in hypercholesterolemia is attenuated by L-arginine. **Circulation** 89(5):2176-82, 1994.

Turko, I. V. e F. Murad. Protein nitration in cardiovascular diseases. **Pharmacol Rev** 54:619-34, 2002.

Vanhoutte PM, Shimokawa H, Tang EHC, Félétou M. Endothelial dysfunction and vascular disease. **Acta Physiol** 196:193–222, 2009.

Vásquez-Vivar J, Kalyanaraman B, Martásek P, Hogg N, Masters BS, Karoui H, Tordo P, Pritchard KA Jr.Superoxide generation by endothelial nitric oxide synthase: the influence of cofactors. **Proc Natl Acad Sci U S A** 95:9220-5, 1998.

Von Harsdorf R, Kang RE, Fullerton M, Woodcock EA. Myocardial stretch stimulates phosphatidyl-inositol turnover. **Circ Res** 65:494-501, 1989.

Wegener JW, Nawrath H, Wolfsgruber W, Kühbandner S, Werner C, Hofmann F, Feil R. cGMP-dependent protein kinase I mediates the negative inotropic effect of cGMP in the murine myocardium. **Circ Res** 90:18–20, 2002.

Wever RM, Lüscher TF, Cosentino F, Rabelink TJ. Atherosclerosis and the two faces of endothelial nitric oxide synthase. **Circulation** 97:108-12, 1998.

Wollert KC, Drexler H. Regulation of cardiac remodeling by nitric oxide: focus on cardiac myocite hypertrophy and apoptosis. **Heart Fail Rev** 7:317-25, 2002.

Wollert KC, Fiedler B, Gambaryan S, Smolenski A, Heineke J, Butt E, Trautwein C, Lohmann SM, Drexler H.Gene transfer of cGMP-dependent protein kinase I enhances the antihypertrophic effects of nitric oxide in cardiomyocytes. **Hypertension** 39:87-92, 2002.

World Health Organization. Facts related to chronic diseases. 2008. site:http//www.who.int/dietphysicalactivity/publications/facts/chronic/en

Xia Y, Tsai AL, Berka V, Zweier JL. Superoxide generation from endothelial nitric-oxide synthase. A Ca2+/calmodulin-dependent and tetrahydrobiopterin regulatory process. **J Biol Chem** 273:25804-8, 1998.

Xu KY, Kuppusamy SP, Wang JQ, Li H, Cui H, Dawson TM, Huang PL, Burnett AL, Kuppusamy P, Becker LC. Nitric oxide protects cardiac sarcolemmal membrane enzyme function and ion active transport against ischemia-induced inactivation. **J Biol Chem** 278(43):41798-803, 2003.

Yao EH, Yu Y, Fukuda N. Oxidative stress on progenitor and stem cells in cardiovascular diseases. **Curr Pharm Biotechnol** 7:101-8, 2006.

Yellin MJ, Brett J. Baum D, Matsushima A, Szabolcs M, Stern D, Chess L. Functional interactions of T cells with endothelial cells: the role of CD40LCD40- mediated signals. **J Exp Med** 182:1857-64, 1995.

Zhang P, Xu X, Hu X, van Deel ED, Zhu G, Chen Y. Inducible nitric oxide synthase deficiency protects the heart from systolic overload-induced ventricular hypertrophy and congestive heart failure. **Circ Res** 100:1089–1098, 2007.

IV. 1. *Cardioprotective mechanism of S-nitroso-N-acetylcysteine via S-nitrosated betadrenoceptor-2 in the LDLr-/- mice.*

Title: Cardioprotective mechanism of S-nitroso-N-acetylcysteine via S-nitrosated betadrenoceptor-2 in the LDLr-/- mice.

Amarylis Claudine Bonito Wanschel (Master degree)[a], Ana Iochabel Soares Moretti (PhD)[b], Alexandre Bruni-Cardoso (Master degree)[C], Hernandes Faustino de Carvalho(PhD)[c], Heraldo Possolo de Souza (PhD)[b], Regina Célia Spadari (PhD)[d], Francisco Rafael Martins Laurindo (PhD)[e] and Marta Helena Krieger (PhD)[a,*]

[a]*Laboratory of Cardiovascular and Department of Anatomy, Cellular Biology and Physiology, State University of Campinas (UNICAMP), Biology Institute, São Paulo, Brazil;* [b]*Laboratory of Medical Investigation (LIM-51) and Department of Emergency Medicine, University of São Paulo School of Medicine (USP), São Paulo, Brazil;* [c]*Laboratory of Extracellular Matrix and Department of Anatomy, Cellular Biology and Physiology, State University of Campinas (UNICAMP), Biology Institute, São Paulo, Brazil;* [d]*Laboratory of Stress Biology and Department of Biosciences, Federal University of São Paulo (UNIFESP), São Paulo, Brazil*

[e]*Vascular Biology Laboratory and Heart Institute (InCor),School of Medicine, University of São Paulo School of Medicine (USP), São Paulo, Brazil*

***Correspondence**: **Name:** Marta Helena Krieger, PhD; **Adress:** Universidade Estadual de Campinas, Instituto de Biologia, Departamento de Anatomia, Biologia Celular e Fisiologia, 255 Monteiro Lobato Street, Laboratory 04 Campinas, SP 13083-970; **Phone:** +55 19 3521-6189; **Fax:** +55 19 3521-6185 and **email:** kriegerm@unicamp.br

ABSTRACT

Previous studies from our group have demonstrated the cardio protective effect of S-nitroso-N-acetylcysteine (SNAC) on dyslipidemic LDLr-/- mice. The present study was designed to investigate whether SNAC treatment produces cardio protective effect via an antioxidant role, and to verify the possible anti-apoptotic role of β2-Adrenergic Receptors (β_2-ARs) in the cardiac remodeling. Ventricular superoxide (O_2^-) and hydrogen peroxide (H_2O_2) generation was measured by *HPLC* methods to allow quantification of dihydroethidium (DHE) products. Ventricular histological sections were stained using terminal dUTP nick-end labeling (TUNEL) to identify nuclei with DNA degradation (apoptosis) and this was confirmed by cleaved caspase-3 protein expression. The findings show that H_2O_2 production and cell apoptosis increased during left ventricular hypertrophy (LVH). SNAC treatment showed reduction of oxidative stress on cardiac remodeling by decreasing H_2O_2 and O_2^- production (65% and 52%, respectively), this which was associated with a decrease in the ratio of p-Ser1177 eNOS/total eNOS. Left ventricle (LV) from SNAC treated mice revealed a 4-fold increase in β_2-AR expression; β_2-ARs-S-nitrosation (β_2-AR-SNO) increased 61%, while apoptosis decreased 70%. These results suggest an anti-oxidant role of SNAC on cardio protection, which is associated with the mediation of β_2-ARs overexpression and β_2-AR-SNO via an anti-apoptotic pathway.

Keywords: NO donnor, apoptosis, left ventricular hypertrophy.

1. INTRODUCTION[1]

Left ventricular (LV) remodeling has been consistently associated with heart failure (HF). It involves critical modifications in the functioning of the heart, as well as both cellular and sub cellular organization [1] and can be triggered by various agents [2]. Initially, these changes can augment cardiac performance, but in the long run, they may progress to a maladaptive response and heart failure. The role of oxidative stress as a pathophysiological mechanism in left ventricular remodeling and its participation in the progression of heart failure is well known [3]. Various studies have demonstrated that oxidative stress can induce most of the changes that contribute to myocardial remodeling, with the production of reactive oxygen species (ROS) resulting in a phenotype characterized by hypertrophy and apoptosis in isolated cardiac myocytes [4]. This apoptosis, or programmed cell death, is one of the mechanisms involved in the transition from LVH to heart failure; it has a major role in cell survival signaling pathways in cardiac hypertrophy [5, 6].

Treatments with $NO^{\bullet}$ donors and S-nitrosothiols (RSNOs) have been implicated in a diverse range of cardioprotective functions and $NO^{\bullet}$ has emerged as an endogenous inhibitor of pathological hypertrophy [7]. Previous studies in low-density lipoprotein-receptor-knockout (LDLr-/-) mice, which develop atheroma and left ventricular hypertrophy after 15 days on a high fat diet, have shown that treatment with an $NO^{\bullet}$ donor S-nitroso-N-Acetylcysteine (SNAC) attenuates plaque development by the suppression of the vascular oxidative stress [8]; moreover, SNAC protects the heart from structural and functional myocardial alterations [9] such as heart arrhythmia, which is due to an increase

Abbreviations: LVH, left ventricular hipertrophy; SNAC, s-nitroso-n-acetylcysteine, β_2-AR, betadrenoceptor-2; DHE, dihydroethidium; EOH 2-hydroxyethidium; E, ethidium; S-NO, S-nitrosation.

in the coupling of β_2-AR to Gi [10]. Furthermore, $NO^{\bullet}$ has been linked to G protein-coupled receptors via S-nitrosation, which is a process of signal transduction resulting from the covalent modification of cysteine residue sites of proteins [11-13] and can stimulate adrenoceptor-beta overexpression [14]. Therefore, we have used this model to assess the role of SNAC in oxidative stress and cell survival in cardiac remodeling, with betadrenoceptor-2 (β_2-ARs) used to indicate involvement of the anti apoptotic pathway.

2. MATERIALS AND METHODS

2.1 Left ventricular hypertrophy model.

Three-month-old male low-density lipoprotein-receptor-deficient (LDLr-/-) mice (24 ± 3 g, n = 60) from Jackson Laboratory (Bar Harbor, ME) were used in the experiments. The experimental protocols were approved by the Institutional Committee for Ethics in Animal Experimentation (CEEA/IB 2044-1– UNICAMP) in agreement with the guidelines of the Brazilian College for Animal Experimentation (COBEA). The male mice 3 months old were randomly allocated to one of 3 groups and received food and water *ad libitum* during 15 days: i) Control LDLr-/- mice fed a standard diet (Nuvital CR1) and injected i.p. with a daily dose of 0.1 ml of PBS (C; n=20); ii) Hypercholesterolemic LDLr-/- mice fed a high fat diet (containing: 20% fat, 1.25% cholesterol and 0.5% cholic acid) and injected i.p. with a daily dose of 0.1 ml PBS (H; n=20) and iii) Hypercholesterolemic LDLr-/- mice fed a high fat diet (containing: 20% fat, 1.25% cholesterol and 0.5% cholic acid) but injected i.p. with a daily dose of 0.51 mmol/Kg of SNAC (H + S; n=20). The mice were anesthetized with xylasine (Coopers, São Paulo, Brazil) and ketamine (Parke-Davis, Argentina), 6 mg/kg and 40 mg/kg, respectively, IP. The heart was gently perfused

with PBS/DTPA buffer composed of (in mM) 7.78 Na_2HPO_4, 2.20 KH_2PO_4, 140 NaCl, and 2.73 KCl, pH 7.4, to remove the remaining blood. The left ventricles were removed and cut into segments, which were used immediately for HPLC analysis, and DHE-derived fluorescence. Other mice left ventricle were used for western blotting analysis and TUNEL assay.

2.2 Synthesis of SNAC and In vitro stability of SNAC solution

The SNAC synthesis process, stability solution as well as calculation of the concentration and dose adopted were performed as described [15].

2.3 Tissue extracts analysis by HPLC (Separation of DHE, 2-hydroxyethidium (EOH), and ethidium).

Left ventricle segments (~3 mm in length) were incubated in 0.5 ml of PBS/DTPA buffer containing 100 µM diethylenetriamine pentaacetic acid (Sigma, St. Louis, MO, USA) (PBS/DTPA) for 15 min in a 1.5-ml Eppendorf vial. A volume of 2.5 µl of DHE 10 mM stock solution was added to the buffer to achieve final concentration of 50 µM, and a final DMSO concentration of 0.5% vol/vol and further incubation in the dark was carried out for 30 min at 37°C. The segments were washed in PBS, transferred to liquid nitrogen, and homogeneized with mortar and pestle. The homogenate was resuspended in acetonitrile (0.5 ml), sonicated (3 cycles at 8 W for 10 s), and centrifuged (12.000 *g* for 10 min at 4°C). The supernatant was dried under vacuum (Speed Vac Plus model SC-110A, Thermo Savant), and the resulting pellets maintained at -20°C in the dark until analysis, when the samples were resuspended in 120 µl PBS/DTPA and injected (100 µl) into the HPLC system. Positive controls, elaboration of this method and HPLC conditions of

analysis, was performed as described previously [16]. Simultaneous detection of DHE and its derived oxidation products (EOH and ethidium) using, respectively, ultraviolet and fluorescence detection, allowed the used of DHE as an internal control during organic extraction. Thus DHE-derived products were expressed as ratio of EOH and ethidium generated per DHE consumed (initial DHE concentration minus remaining DHE; EOH/DHE and ethidium/DHE, respectively). The data were also normalized for tissue weight.

2.4 Western blotting

The frozen left ventricular tissue of the mice was pulverised in liquid nitrogen with a mortar and pestle, it was then resuspended in homogenization buffer, 1% Triton X-100 (Amresco, Solon, Ohio), 10mmol/l sodium pyrophosphate, 100mmol/l sodium fluoride, 10µg/ml Aprotinin (Amresco, Solon, Ohio), 1mmol/l PMSF, 0.25mmol/l sodium orthovanadate and 0.1% cocktail inhibitors protease. The samples were centrifuged for 20 min at 11,000g, and the supernatant was collected and assayed for total protein concentration using a Bradford method (Bio Rad, Hercules, CA, USA). Samples were stored at −80°C until assay. Protein expression was determined via SDS-polyacrylamide gel electrophoresis under reducing conditions. Left ventricular tissue extracts (30 µg/ml) from at least four animals of each group were boiled in equal volumes of loading buffer (150 mM Tris-HCl, pH 6.8; 4% SDS; 20% glycerol; 15% β-mercaptoethanol; and 0.01% bromophenol blue) and subjected to electrophoresis on 10% polyacrylamide gels. Following electrophoretic separation, proteins were transferred to Hybond-P membranes (Amersham Pharmacia Biotech, Buckinghamshire, England). Membranes were blocked with 5% non-fat dry milk or bovine serum albumin (Sigma, St. Louis, MO, USA) in buffer

containing 10 mM Tris–HCl (pH 7.6), 10 mM NaCl, and 0.1% Tween 20 (Calbiochem, Darmstadt, Germany) (TBST) for 1 h. Primary antibodies against the following were employed: eNOS (rabbit polyclonal, 1:1000, 610299; BD Transduction Laboratories); eNOSpS1177 (mouse monoclonal, 1:500, 612392; BD Transduction Laboratories); betadrenoceptor-1 (rabbit polyclonal, 1:100, sc-568, Santa Cruz Biothecnology, Santa Cruz, CA, USA), betadrenoceptor-2 (rabbit polyclonal,1:100, sc570, Santa Cruz Biothecnology, Santa Cruz, CA, USA), caspase-3 (rabbit polyclonal, 1:1000, sc7148, Santa Cruz Biothecnology, Santa Cruz, CA, USA), nitrotyrosine (mouse monoclonal, 1:1000, clone 1A6), and GAPDH (rabbit polyclonal, 1:2.000, sc25778, Santa Cruz Biothecnology, Santa Cruz, CA, USA), all antibodies were incubated at 4°C overnight. After the blots had been washed twice with TBST, secondary antibody horseradish peroxidase conjugate (goat anti-rabbit polyclonal, 1:10.000, G21234 or goat anti-mouse 81-6520, Invitrogen, Molecular Probes, Oregon, USA) was applied at 1:10.000 for 1 h. Blots were washed in TBST twice over 30 min, incubated using an enhanced Super Signal chemiluminescent reagent detection kit (Pierce, Rockford, IL, USA), and exposed to Kodak O-OMAT-AR photographic film (Kodak, Rochester, NY, USA). Band intensity of original blots was quantified using Image J software.

2.5 Assessment of S-nitrosation using chemical derivatization Biotin-switch (BST) coupled to immunoprecipitation and Western blotting

S-nitrosated proteins were labeled with biotin in the lysates, as previously described [17, 18]. Left ventricles were rinsed with PBS containing 0.1 mM EDTA and 0.01 mM neocuproine (Sigma, St. Louis, MO, USA), cut into segments, which were pulverised in liquid nitrogen with a mortar and pestle, immediately resuspended in HEN lyses buffer

containing 0.1% SDS, 0.5% CHAPS, and 20 mM NEM (N-ethylmaleimide) (Sigma, St. Louis, MO, USA), and lysed by rocking for 30 min, at 4 C. The lysates were centrifuged for 10 min at 14,000g and 4 C, and the excess NEM used to block sulfhydryl groups (SH) was removed by protein precipitation with acetone. The resulting pellets were resuspended in HEN buffer containing 1% SDS (HENS), and the S-nitrosothiols were reduced and biotinylated by the simultaneous addition of 10 mM sodium ascorbate and 0.05 mM of the sulfhydryl-specific biotinylating agent, MPB [N-(3-maleimidylpropionyl) biocytin, Molecular Probes], for 1 h at room temperature (RT). The extra label was removed by a second acetone precipitation, and the proteins resuspended in HENS buffer for immunoprecipitation of β_2-adrenoceptor-2 (anti-rabbit β_2-AR). Biotinylation of betadrenoceptor-2 and pro-caspase3 was detected by immunoprecipitation. Left ventricular tissue extracts (100µg/ml) were incubated overnight in 50µl streptavidin–HRP. Immunoprecipitates were washed three times with 800 µL of HEN buffer and resuspended in 25 µL of HEN, followed by the addition of 20 µL of 2 Laemmli sample buffer (150 mM Tris-HCl, pH 6.8; 4% SDS; 20% glycerol and 0.01% bromophenol blue) and boiling at 95 C for 5 min; western blotting was then performed as described above. Control experiments were also performed in which the sodium ascorbate was omitted, thus preventing the reduction of S-nitrothiols. All samples were protected from light during all procedures prior to electrophoresis; densities were analyzed by Image J software.

2.6 DNA fragmentation detection by Terminal deoxynucleotidyl transferase mediated - dUTP nick end labeling (TUNEL)

Each left ventricle was weighed, and the ratio of LV weight (mg) per body weight (g) was calculated. Briefly the mice were anesthetized, and their hearts were perfused in

situ with PBS followed by 10% PBS buffered formaldehyde. The LVs were fixed in 10% formaldehyde for at least 2 days and then washed in 70% alcohol, they were then processed for paraffin inclusion using standard methods; cross-sections of 3 µm were cut and mounted on silanized glass slides, dewaxed with xylene, and rehydrated in a decreasing ethanol series. Endogenous peroxidase activity was blocked with 3% hydrogen peroxide in water for 30 minutes and assayed for DNA fragmentation using a TUNEL assay (In Situ Cell Death Detection Kit, POD- Roche Mannheim, Germany) according to the manufacturer's instructions. After extension of the fluorescein-labeled deoxy-UTP tail with the TdT enzyme, a peroxidase-labeled anti-fluorescein antibody was used and peroxidase activity was revealed with 3,30-diaminobenzidine. Twenty microscopic fields from the LV of three animals per group were selected randomly at 100x objective. The frequency of apoptotic cells was counted and expressed as a percentage of the total. Observations and photomicrographs were made with an Olympus microscope equipped for fluorescence microscopy.

3. RESULTS

3.1 ROS species reduction and eNOS activation

HPLC analysis and quantification of the DHE-derived fluorescent products may increase our understanding of redox events during LVH remodeling. HPLC analysis of the left ventricle revealed an increase of 47% in the ethidium/DHE ratio for the hypertrophied left ventricles from animals of the H group than those in the control group. SNAC treatment revealed decreased ratios of ethidium/DHE and EOH/DHE (%65 and 52% respectively) in relation to those of the H group (Figure 1a).

The ratio of p-Ser1177 eNOS/ total eNOS on left ventricle from control and H mice were not changed. However, the SNAC treatment revealed aproximadely 50% of reduction on this ratio on H+ S mice, as seen in Figure 1b.

To exclude the participation of the $NO^{\bullet}$ donor- SNAC into the oxidative environment which could result on peroxynitrite formation, we analyzed nitrotyrosine (NT) expression used as a biomarker of reactive nitrogen species formation [19]. No changes on NT expression on the left ventricle from animals treated with SNAC compared with H group were observed (Figure 1c).

3.2 β-adrenoceptors involvement

To investigate the pathway mediating this pro-apoptotic effect in the cardiomyocytes of the left ventricle, we first analyzed initial β_1-AR expression, and found no significant differences (Figure 2). We then evaluated β_2-AR protein expression to verify the effects of SNAC treatment in the mediation of the anti-apoptotic effect. We found that

15 days on a high fat diet (LVH) plus treatment with SNAC lead a 4-fold increase in β_2-AR expression (P <0.001; n =7; Figure 2).

3.3 β-adrenoceptors S-nitrosation

Because S-nitrosothiols (RSNOs) is reported modulate G-protein coupled receptor signaling via reversible, thiol-sensitive mechanisms we assessed the S-nitrosation status of β_2-AR at cysteine residue in heart tissue by biotin-switch followed immunoprecipitation and western blotting. Left ventricle were subjected to the biotin-switch and probed for S-nitrosated GAPDH (GAPDH–SNO), along with ascorbate control (Figure 3a). Notably, omission of ascorbate leads to nearly complete loss of biotinylation signal. β_2-AR nitrosation in the H + S group exceeded that in the H group by 61% (Figure 3b).

3.4 Inhibition of apoptosis

To investigate the viability of myocardial cells in the left ventricle regions, and the *in vivo* anti-apoptotic effect of SNAC, we performed TUNEL staining on the different experimental groups. Representative photographs of TUNEL-positive nuclei in the heart are shown in Figure 4a. Quantitative analysis showed a significantly higher proportion of TUNEL-positive cells in the myocardium of H mice than in that of control mice, whereas very few or no TUNEL-positive cells could be detected in the hearts the H mice after SNAC treatment (Figure 4b). These cell apoptosis results were confirmed by western blotting with specific antibody of cleaved caspase-3 (Figure 4c). Cell apoptosis was confirmed by cleaved caspase-3 protein expression, since these increases in response to diverse intrinsic and extrinsic death stimuli. As expected, LVH increased levels of cleaved caspase-3 in the protein mouse hearts (Figure 4c). However, this increase was significantly blocked by treatment with SNAC. To confirm the protective effect of SNAC may be partially mediated through the inhibition of caspase-3 activity by $NO^{\bullet}$ -mediated *S*-

nitrosation we assessed S-nitrosation of procaspase-3 and caspase-3 cleaved. The results indicate that the protective effect of SNAC from $NO^{\bullet}$ donation cannot be partially $NO^{\bullet}$-mediated caspase-3 *S*-nitrosation (Figure 5).

4. DISCUSSION

This study has investigated the cardio protective role of SNAC against of oxidative stress as well as its role in cell survival in the hypertrophied heart. We identified an increased β2-ARs nitrosated which may explain the anti-apoptotic effect of SNAC treatment. This proposal was derived from previous studies using the same animal model that showed, firstly, that SNAC treatment exerts an anti-oxidant effect by suppressing superoxide overproduction in the aorta [8] and a protective effect in structural and functional myocardial alterations [9]. Moreover, this myocardial effect protecting the heart from arrhythmia [10] was due to the induction of an increase in β_2-AR coupling to Gi.

Our findings have demonstrated increased oxidative stress in left ventricle hypertrophy, demonstrated by H_2O_2 in the LV of LDLr-/- mice fed a high fat diet. However, DHE oxidized to a compound characterized as ethidium represents the overlapping of oxidation products due to specific (H_2O_2) and nonspecific sources (heme proteins) [20, 21]. The development of oxidative stress in the LVH is a multifactorial process caused by variety of mechanisms. Superoxide anions are probably the most important free oxygen radical generated *in vivo*, and it is highly likely that they are derived from more than one source. One major source is NADPH oxidase, but ROS can also be produced intracellularly through electron leakage from the mitochondria during oxidative phosphorylation and through the activation of various cellular enzymes, including xanthine oxidase, nitric oxide synthase uncoupling and/or cyclooxygenase [22-26]. Superoxide is subject to dismutation by superoxide dismutase (SOD) into H_2O_2, a compound which may mediate the compensatory responses involved in cardiac remodeling. Previous studies [9] in this animal model have shown that SNAC is able to suppress cardiac remodeling; and in the present study we have demonstrated that these effects are due to suppression of ROS

generation in the LV of LDLr-/- mice fed high fat diet. Similar levels in the cardiac remodeling of the ROS reduction by antioxidants have been shown *in vivo* [27, 28]. We suggest that this reduction may be due to the well known scavenging action of RSNOs or the N-acetylcysteine *per se* activity as antioxidant *in vivo* and *in vitro*. N-acetylcysteine also reacts with hydroxyl radical with a rate constant of 1.36 X 10(10) $M^{-1}s^{-1}$ [29]. It also reacts slowly with H_2O_2 and superoxide (O_2^-).

One novel finding of the present study was that in the myocardium oxidative stress of the LV decreased due to SNAC treatment, concomitant with ratio of p-Ser1177 eNOS/ total eNOS reduction. These results may suggest that elevated ROS levels stimulate eNOS activation. Similar findings in other models indicate the induction of eNOS phosphorylation by H_2O_2 and its consequent activation [30-33] through an Akt-phosphorylation-dependent pathway [32]. Previous studies of the aorta of these animals showed that the location of the elevated superoxide levels is associated with constitutive NOS overexpression levels [8]. We believe that possible explanation for the ratio of p-Ser1179 eNOS/ total eNOS reduction by $NO^{\bullet}$ donor SNAC treatment may be due feedback mechanism.

The cardioprotective action of SNAC in the left ventricle (LV) can be attributed to the induction of the overexpression of β_2-AR. S-nitrosothiols are known to induce betadrenoceptor overexpression, and these RSNO are able to prevent agonist-stimulated receptor downregulation [14]. Whereas, have been described that activation of the β_2AR protects myocytes against apoptosis induced by a wide array of assaulting factors, such enhanced β_1AR signaling, hypoxia, and ROS [34-36]. However, this overexpression can be associated with changes in coupling mechanisms. β_2-AR is a member of the class A-family

of GPCRs that may couple pathway via both Gs- and Gi-proteins. Treatment with SNAC leads to the coupling of β_2-AR to Gi, a mechanism which prevents arrhythmia. Also, the activation of β_2AR-coupled Gi protects cardiac myocytes from apoptosis via downstream target (PI3K)-AKT (also known as protein kinase B) survivor pathway [34, 35]. This kind of coupling change on G-protein from β_2-adrenergic receptor mechanism was induced by 3-morpholinosydnonimine (SIN-1), which releases $NO^{\bullet}$ and superoxide simultaneously [37]. The TUNEL-positive cells showed progressive and significant increase in myocyte apoptosis from LV on H mice and these findings suggest that in these cardiac remodeling occurred myocyte apoptosis as others studies have been shown [38, 39]. Cardiomyocyte apoptosis increased 70% during LVH; the prevention of cardiac remodeling by SNAC treatment lead to a decrease in the number of apoptotic cardiomyocytes. We thus suggest that, SNAC protects cardiomyocytes from apoptosis via activation of the β_2AR-coupled Gi pathway.

The present study has shown that SNAC treatment increases S-nitrosation in the β_2-AR. It has been recognized that S-nitrosation (cGMP-independent) reactions can modulate a wide range of cell functions [40, 41]. It is result of the covalent modification of Cys thiols which are important in cardio protection [42-44]. To our knowledge, this is the first finding of β_2AR S-nitrosation. We understand the modification of this protein as evidence of coupling change. This is in agreement with these results of studies from Adam *et al.* [37] showing $NO^{\bullet}$ effects on the depalmitoylation of β_2AR, including the reduction of the potency of a β-adrenergic agonist in the stimulating of adenylyl cyclase uncoupling β_2AR to Gs pathway. Indeed, we have demonstrated that SNAC treatment promotes β_2AR-Gs uncoupling and Gi coupling and with the present data we suggest that this phenomenon

may be mediated by β_2AR-SNO. Therefore, we investigated the mechanism of caspase inhibition, which is reported that caspases are also reversibly inhibited by $NO^{\bullet}$ related *S*-nitrosation [45]. The caspases are a family of cysteine proteases and $NO^{\bullet}$ can modify enzyme function by *S*-nitrosation of protein thiol groups [41, 46]. However our findings did not show differences in the S-nitrosated status of the procaspase-3 $NO^{\bullet}$ donation from SNAC treatment.

In conclusion, the present study has for the first time demonstrated, that administrations of SNAC suppress cardiac remodeling on LDLr-/- mice fed high fat diet via the inhibition of oxidative stress, and apoptosis which are result of β_2AR overexpression and the coupling changes thought about by nitrosation.

Acknowledgments

The authors would like to acknowledge the financial support of the CAPES and the technical assistance of Maria A. Bertoline.

5. REFERENCES

[1] B. Swynghedauw, Molecular mechanisms of myocardial remodeling. Physiol. Rev. 79 (1999) 215-62.

[2] R.D. Brown, S.K. Ambler, M.D. Mitchel, C.S. Long, The cardiac fibroblast: therapeutic target in myocardial remodeling and failure. Annual Review of Pharmacology and Toxicology 45 (2005) 657-687.

[3] H. Tsutsui, S. Kinugawa, S. Matsushima, Mitochondrial oxidative stress and dysfunction in myocardial remodeling. Cardiovascular Research 81 (2008) 449–456.

[4] F.G. Spinale, M.L. Coker, C.V. Thomas, J.D. Walker, R. Mukherjee L. Hebbar, Time-dependent changes in matrix metalloproteinase activity and expression during the progression of congestive heart failure: relation to ventricular and myocyte function. Circ Res. 82 (1998) 482–495.

[5] B. Ding, R.L. Price, E.C. Goldsmith, T.K. Borg, X. Yan, P.S. Douglas, E.O. Weinberg, J. Bartunek, T. Thielen, V.V. Didenko, B.H. Lorell, Left ventricular hypertrophy in ascending aortic stenosis mice: anoikis and the progression to early failure. Circulation 101 (2000) 2854-62.

[6] E. Palojoki, A. Saraste, A. Eriksson, K. Pulkki, M. Kallajoki, L.M. Voipio-Pulkki, I.Tikkanen, Cardiomyocyte apoptosis and ventricular remodeling after myocardial infarction in rats. Am. J. Physiol. Heart Circ. Physiol. 280 (2001) H2726–H2731.

[7] L.A. Barouch, T.P. Cappola, R.W. Harrison, J.K. Crone, E.R. Rodriguez, A.L. Burnett, J.M. Hare, Combined loss of neuronal and endothelial nitric oxide synthase causes premature mortality and age related hypertrophic cardiac remodeling in mice. J Mol Cell Cardiol. 35 (2003) 637–644.

[8] M.H. Krieger, K.F.R. Santos, S.M. Shishido, A.C. Wanschel, H.F. Estrela, L. Santos, M.G. De Oliveira, K.G. Franchini, , R.C. Spadari-Bratfisch, F.R.M. Laurindo, Antiatherogenic effects of S-nitroso-N-acetylcysteine in hypercholesterolemic LDL receptor knockout mice. Nitric Oxide 14 (2006) 12–20.

[9] J.A.D. Garcia, L. Santos, A.L. Moura, K.F.S. Ricardo, A.C.B.A. Wanschel, S.M. Shishido, R.C. Spadari-Bratfisch, H.P. de Souza, M.H. Krieger, S-Nitroso-N-Acetylcysteine (SNAC) Prevents Myocardial Alterations in Hypercholesterolemic LDL Receptor Knockout Mice by Antiinflammatory Action. J Cardiovasc Pharmacol. 51 (2008) 78-85.

[10] V.M. Caceres, A.L. Moura, A.C.B.A.Wanschel, M. H. Krieger, R.C. Spadari, Coupling of beta-2 adrenoceptors to inhibitory G protein in atria of hypercholesterolemic LDLr-/- mice. *Brit* Pharmacol. *"Unpublished results"*.

[11] D.T. Hess, A. Matsumoto, S.O. Kim, H.E. Marshall, J.S. Stamler, Protein S-nitrosylation: purview and parameters. Nat. Rev. Mol. Cell Biol. 6 (2005) 150–166.

[12] E.J. Whalen, M.W. Foster, A. Matsumoto, K. Ozawa, J.D. Violin, L.G. Que, C.D. Nelson, M. Benhar, J.R. Keys, H.A. Rockman, W.J. Koch, Y. Daaka, R.J. Lefkowitz, S.J. Stamler, Regulation of β-Adrenergic Receptor Signaling by S-Nitrosylation of G-Protein-Coupled Receptor Kinase 2. Cell 129 (2007) 511–522.

[13] T. Kokkola, J.R. Savinainen, K.S. Monkkonen, M.D. Retamal, J.T. Laitinen, S-nitrosothiols modulate G protein-coupled receptor signaling in a reversible and highly receptor-specific manner. BMC Cell Biol. 6 (2005) 1-17.

[14] E.J. Whalen, A.K. Johnson, S.J. Lewis, ß-Adrenoceptor Dysfunction After Inhibition of NO Synthesis. Hypertension 36 (2000) 376-382.

[15] K.F. Ricardo, S.M. Shishido, M.G. de Oliveira, M.H. Krieger, Characterization of the hypotensive effect of S-nitroso-N-acetylcysteine in normotensive and hypertensive conscious rats. Nitric Oxide 7 (2002) 57-66.

[16] D.C. Fernandes, J.Jr. Wosniak, L.A. Pescatore, M.A. Bertoline, M. Liberman, F.R. Laurindo, C.X. Santos, Analysis of DHE-derived oxidation products by HPLC in the assessment of superoxide production and NADPH oxidase activity in vascular systems. Am J Physiol Cell Physiol. 292 (2007) C413-22.

[17] S.R. Jaffrey, S.H. Snyder, The biotin-switch method for the detection of S-nitrosylated proteins. Sci. Stroke 86 (2001) pl1.

[18] M.T. Forrester, M.W. Foster, M. Benhar, J.S. Stamler, Detection of protein S-nitrosylation with the biotin-switch technique. Free Radic Biol Med. 46 (2009)119-26.

[19] I.V. Turko, F. Murad, Protein nitration in cardiovascular diseases. Pharmacol Rev. 54 (2002) 619-34.

[20] I. Papapostolou, N. Patsoukis, C.D. Georgiou, The fluorescence detection of superoxide radical using hydroethidine could be complicated by the presence of heme proteins. Anal Biochem. 332 (2004) 290–298.

[21] H. Zhao, J. Joseph, H.M. Fales, E.A. Sokoloski, R.L. Levine, J. Vasquez- Vivar, B. Kalyanaraman, Detection and characterization of the product of hydroethidine and intracellular superoxide by HPLC and limitations of fluorescence. Proc Natl Acad Sci U.S.A. 102 (2005) 5727–5732.

[22] C. Heymes, J.K. Bendall, P. Ratajczak, A.C. Cave, J.L. Samuel, G. Hasenfuss, A.M. Shah, Increased myocardial NADPH oxidase activity in human heart failure. J Am Coll Cardiol. 41 (2003) 2164–71.

[23] K. Nakamura, K. Kusano, Y. Nakamura, M. Kakishita, K. Ohta, S. Nagase, M. Yamamoto, K. Miyaji, H. Saito, H. Morita, T. Emori, H. Matsubara, S. Toyokuni, T. Ohe, Carvedilol decreases elevated oxidative stress in human failing myocardium. Circulation 105 (2002) 2867–71.

[24] U. Landmesser, S. Spiekermann, S. Dikalov, H. Tatge, R. Wilke, C. Kohler, D.G. Harrison, B. Hornig, H. Drexler, Vascular oxidative stress and endothelial dysfunction in patients with chronic heart failure: role of xanthine-oxidase and extracellular superoxide dismutase. Circulation 106 (2002) 3073–8.

[25] C.A. Farquharson, R. Butler, A. Hill, J.J. Belch, A.D. Struthers, Allopurinol improves endothelial dysfunction in chronic heart failure. Circulation 106 (2002) 221–6.

[26] Y. Shizukuda, P.M. Buttrick, Oxygen free radicals and heart failure: new insight into an old question. Am J Physiol Lung Cell Mol Physiol. 283 (2002) 237–238.

[27] D.J. Chess, W. Xu, R. Khairallah, K.M. O'Shea, W.J. Kop, A.M. Azimzadeh, W.C. Stanley, The antioxidant tempol attenuates pressure overload-induced cardiac hypertrophy and contractile dysfunction in mice fed a high-fructose diet. Am J Physiol Heart Circ Physiol. 295 (2008) H2223–H2230.

[28] M.O. Date, T. Morita, N. Yamashita, K. Nishida, O. Yamaguchi, Y. Higuchi, S. Hirotani, Y. Matsumura, M. Hori, M. Tada, K. Otsu, The Antioxidant N-2 Mercaptopropionyl Glycine Attenuates Left Ventricular Hypertrophy in In Vivo Murine Pressure Overload Model. J Am Coll Cardiol. 39 (2002) 907-12.

[29] O.I. Aruoma, B. Halliwell, B.M. Hoey, J. Butler, The antioxidant action of N-acetylcysteine: its reaction with hydrogen peroxide, hydroxyl radical, superoxide, and hypochlorous acid. Free Radic Biol Med. 6 (1989) 593-7.

[30] G.R. Drummond, H. Cai, M.E. Davis, S. Ramasamy, D.G. Harrison, Transcriptional and posttranscriptional regulation of endothelial nitric oxide synthase expression by hydrogen peroxide. Circ. Res. 86 (2000) 347–354.

[31] H. Cai, M.E. Davis, G.R. Drummond, D.G. Harrison, Induction of endothelial NO synthase by hydrogen peroxide via a Ca(2+)/calmodulin-dependent protein kinase II/janus kinase 2-dependent pathway. Arterioscler. Thromb. Vasc. Biol. 21 (2001) 1571–1576.

[32] S.R. Thomas, K. Chen, J.F.Jr. Keaney, Hydrogen Peroxide Activates Endothelial Nitric-oxide Synthase through Coordinated Phosphorylation and Dephosphorylation via a Phosphoinositide 3-Kinase-dependent Signaling Pathway. J. Biol. Chem. 277 (2002) 6017–6024.

[33] H. Cai, Z. Li, S. Dikalov, S.M. Holland, J.Jo.H. Hwang, S.C.Jr. Dudley, D.G.Harrison, NAD(P)H oxidase-derived hydrogen peroxide mediates endothelial nitric oxide production in response to angiotensin II.J Biol Chem. 50 (2002) 48311-7.

[34] A. Chesley, M.S. Lundberg, T. Asai, R.P. Xiao, S. Ohtani, E.G. Lakatta, M.T.Crow, The β2-adrenergic receptor delivers an antiapoptotic signal to cardiac myocytes through Gi-dependent coupling to phosphatidylinositol 3'-kinase. Circ. Res. 87 (2000) 1172-1179.

[35] W.Z. Zhu, M. Zheng, W.J. Koch, R.J. Lefkowitz, B.K. Kobilka, R.P. Xiao, Dual modulation of cell survival and cell death by β2-adrenergic signaling in adult mouse cardiac myocytes. Proc. Natl. Acad. Sci. U.S.A. 98 (2001) 1607-1612.

[36] C. Communal, K. Singh, D.B. Sawyer, W.S. Colucci, Opposing effects of β1- and β2-adrenergic receptors on cardiac myocyte apoptosis: Role of a pertussis toxin-sensitive G protein. Circulation 100 (1999) 2210-2212.

[37] L. Adam, M. Bouvier, T.L. Jones, Nitric oxide modulates beta (2)-adrenergic receptor palmitoylation and signaling. J Biol Chem. 37 (1999) 26337-43.

[38] M. Sun, M. Chen, F. Dawood, U. Zurawska, J.Y. Li, T. Parker, Z. Kassiri, L.A. Kirshenbaum, M. Arnold, R. Khokha, P.P. Liu, Tumor necrosis factor-alpha mediates cardiac remodeling and ventricular dysfunction after pressure overload state. Circulation 115 (2007) 1398-407.

[39] G. Condorelli, C. Morisco, N.A. Stassi, F. Farina, G. Sgaramella, A. de Rienzo, R. Roncarati, B. Trimarco, G. Lembo, Increased cardiomyocyte apoptosis and changes in proapoptotic and antiapoptotic genes bax and bcl-2 during left ventricular adaptations to chronic pressure overload in the rat. Circulation 99 (1999) 3071-8.

[40] M.C. Broillet, S-Nitrosylation of proteins. Cellular and Molecular Life Sciences 55 (1999) 1036–1042.

[41] J.S. Stamler, S. Lamas, F.C. Fang, Nitrosylation: the prototypic redox-based signaling mechanism. Cell 106 (2001) 675–683.

[42] J. Lin, C. Steenbergen, E. Murphy, J. Sun, Estrogen receptor-b activation results in S-nitrosylation of proteins involved in cardioprotection. Circulation 120 (2009) 245–254.

[43] J. Sun, E. Picht, K.S. Ginsburg, D.M. Bers, C. Steenbergen E. Murphy, Hypercontractile female hearts exhibit increased S-nitrosylation of the L-type Ca21 channel a1 subunit and reduced ischemia/reperfusion injury. Circ Res. 98 (2006) 403– 411.

[44] S. Atar, Y. Ye, Y. Lin, S.Y. Freeberg, S.P. Nishi, S. Rosanio, M.H. Huang, B.F. Uretsky, J.R. Perez-Polo, Y. Birnbaum, Atorvastatin-induced cardioprotection is mediated by increasing inducible nitric oxide synthase and consequent S-nitrosylation of cyclooxygenase-2. Am J Physiol Heart Circ Physiol. 290 (2006) H1960–H1968.

[45] J. Li, T.R. Billiar, R.V. Talanian, Y.M. Kim, Nitric oxide reversibly inhibits seven members of the caspase family via S-nitrosylation. Biochem Biophys Res Commun. 17 (1997) 419-24.

[46] J.S. Stamler, Redox signaling: nitrosylation and related target interactions of nitric oxide. Cell 23 (1994) 931-6.

Figure Legends

Figure 1. **Production of reactive oxygen species in left ventricle.** Mice after fifteen days of treatment with chow diet injected i.p. with a daily dose of 0.1 ml of PBS (C), hipercholesterolemic diet injected i.p. with a daily dose of 0.1 ml of PBS (H) and hipercholesterolemic diet injected i.p. with a daily dose of 0.1 ml of SNAC (H+S). (a) Ratio of 2-hydroxyethidium/diihydroethidium (EOH/DHE) and ethidium/diihydroethidium (E/DHE). Values are means ± SE (n = animals per group). The same letters indicate the comparisons that are significantly different. $^{a,b,d}P<0.001$ and ^{c} $P<0.01$. (b) Phosphorylated and unphosphorylated endothelial nitric oxide synthase (eNOSpSer1177 and eNOS) protein expression. Phosphorylated proteins were quantified by densitometry and expressed as percentage of change, in relation to unphosphorylated proteins and GAPDH, expressed as (%C). Values are means ± S.E.M. for at least four animals in each group, Anova + Tukey test. (c) Nitrotyrosine protein expression. Proteins were quantified by densitometry and expressed in relation to GAPDH protein. Values are means ± S.E.M. for at least four animals in each group, (ANOVA, *P*=NS).

Figure 2. **Betadrenoceptor-1 (β-$_1$AR) and betadrenoceptor-2 (β-$_2$AR) protein expression.** Left ventricle (LV) of mice after fifteen days of treatment with chow diet injected i.p. with a daily dose of 0.1 ml of PBS (C), hypercholesterolemic diet injected i.p. with a daily dose of 0.1 ml of PBS (H) and hypercholesterolemic diet injected i.p. with a daily dose of 0.1 ml of SNAC (H+S). Proteins were quantified by densitometry and expressed as percentage of change, in relation to GAPDH protein, and (%C). Diffrences between* *vs*. **, * *vs*. † were significant ($p<0.001$). Values are means ± S.E.M. for at least four animals in each group, Anova + Tukey test.

Figure 3. **Typical Biotin Switch (BST) detects both endogenous and exogenous S-nitrosation in left ventricular tissue.** (a) Left ventricle were subjected to the BST and probed for S-nitrosated GAPDH (GAPDH–SNO), along with ascorbate control. Notably, omission of ascorbate leads to nearly complete loss of biotinylation signal. Left ventricular tissue was subjected to the BST and biotinylation reaction (~100 μg) was analyzed by immunoblotting with avidin–HRP and anti-GAPDH antibody (for input). (b) BST in left ventricle (LV) of mice after fifteen days of treatment with hipercholesterolemic diet injected i.p. with a daily dose of 0.1 ml of PBS (H) and hipercholesterolemic diet injected i.p. with a daily dose of 0.1 ml of SNAC (H+S). SNAC- increased β-$_2$ AR S-nitrosated proteins. An aliquot (100 μg) of whole tissue lysates from were immunoblotted with avidin–HRP and anti-betadrenoceptor2-. β-$_2$ AR and GAPDH were shown to indicate equal amount of proteins loaded, and expressed as percentage of compared H group. Data are presented as mean±S.D. for four experiments.

Figure 4. **Apoptosis.** After fifteen days of treatment with chow diet injected i.p. with a daily dose of 0.1 ml of PBS (C), hipercholesterolemic diet injected i.p. with a daily dose of 0.1 ml of PBS (H) and hipercholesterolemic diet injected i.p. with a daily dose of 0.1 ml of SNAC (H+S). (a) Representative photographs of TUNEL-stained histological heart sections from left ventricle (LV) of mice showing apoptotic nuclei. Bar = 10μm. (b) Index of apoptotic cells per field expressed as percentage of apoptotic/total cells ratio. Diffrences between * *vs*. †, ** *vs*. † were significant (p<0.05) and * *vs*. ** were significant (p<0.001). (c) Procaspase-3 protein expression, tissue of LV were quantified by densitometry and expressed as percentage of change, in relation to GAPDH protein. Values are means ± S.E.M. for at least three animals in each group, Anova + Tukey test.

Figure 5. **Typical Biotin Switch (BST) detects both endogenous and exogenous S-nitrosation in left ventricle tissue.** After fifteen days of treatment with chow diet injected i.p. with a daily dose of 0.1 ml of PBS (C), hipercholesterolemic diet injected i.p. with a daily dose of 0.1 ml of PBS (H) and hipercholesterolemic diet injected i.p. with a daily dose of 0.1 ml of SNAC (H+S).Values are means ± S.E.M. for at least four animals in each group, (ANOVA, *P*=NS). Left ventricular tissue was subjected to the BST and biotinylation reaction and aliquot (~100 μg) of whole tissue lysates was analyzed by immunoblotting with avidin–HRP and anti-caspase-3 (for input).

Figure 1.

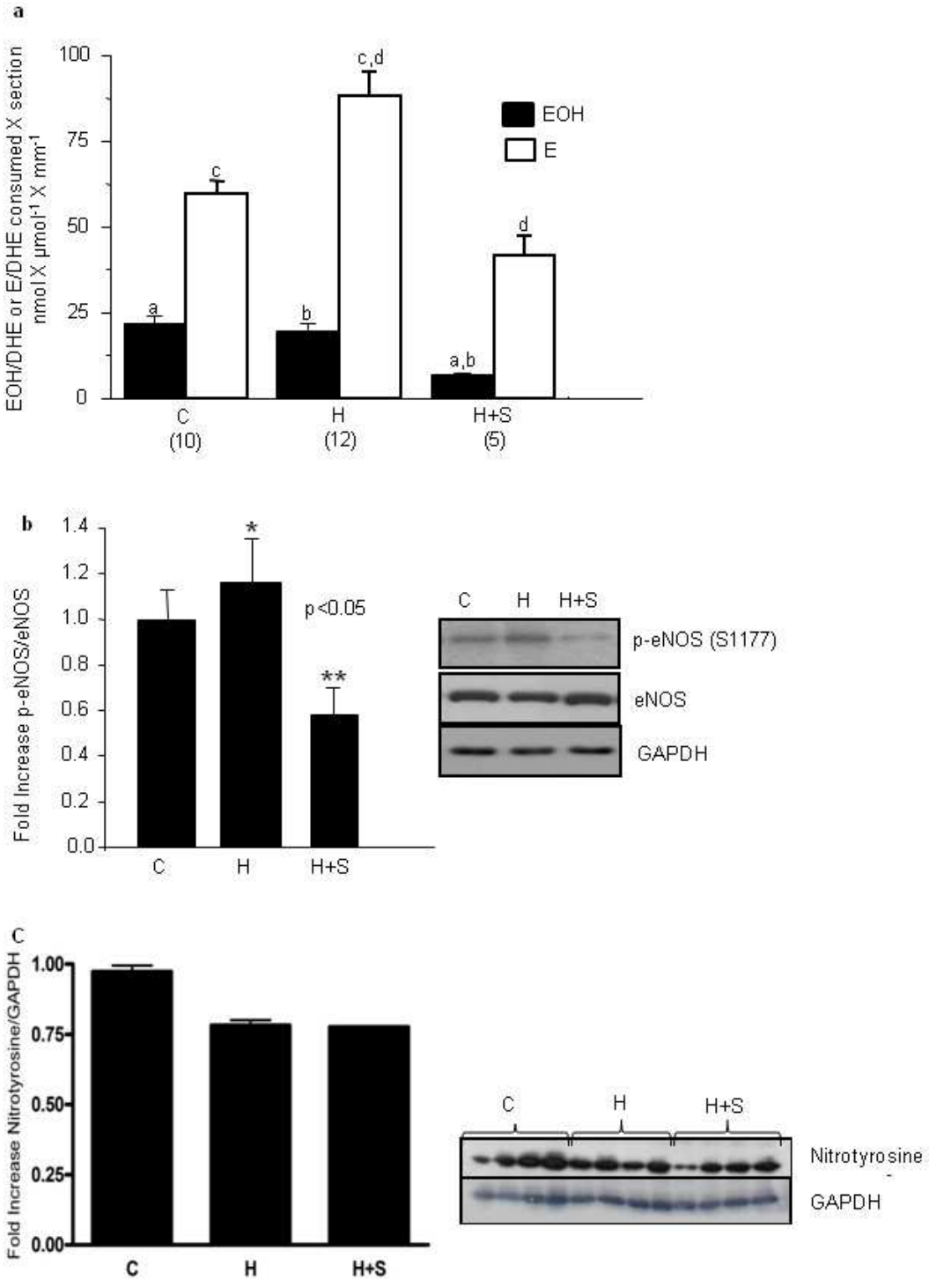
a
EOH/DHE or E/DHE consumed X section
nmol X µmol-1 X mm-1
100
75
50
25
0
a
c
b
c,d
a,b
d
EOH
E
C
(10)
H
(12)
H+S
(5)
b
Fold Increase p-eNOS/eNOS
1.4
1.2
1.0
0.8
0.6
0.4
0.2
0.0
*
**
p<0.05
C
H
H+S
C H H+S
p-eNOS (S1177)
eNOS
GAPDH
C
Fold Increase Nitrotyrosine/GAPDH
1.00
0.75
0.50
0.25
0.00
C
H
H+S
C H H+S
Nitrotyrosine
GAPDH

Figure 2.

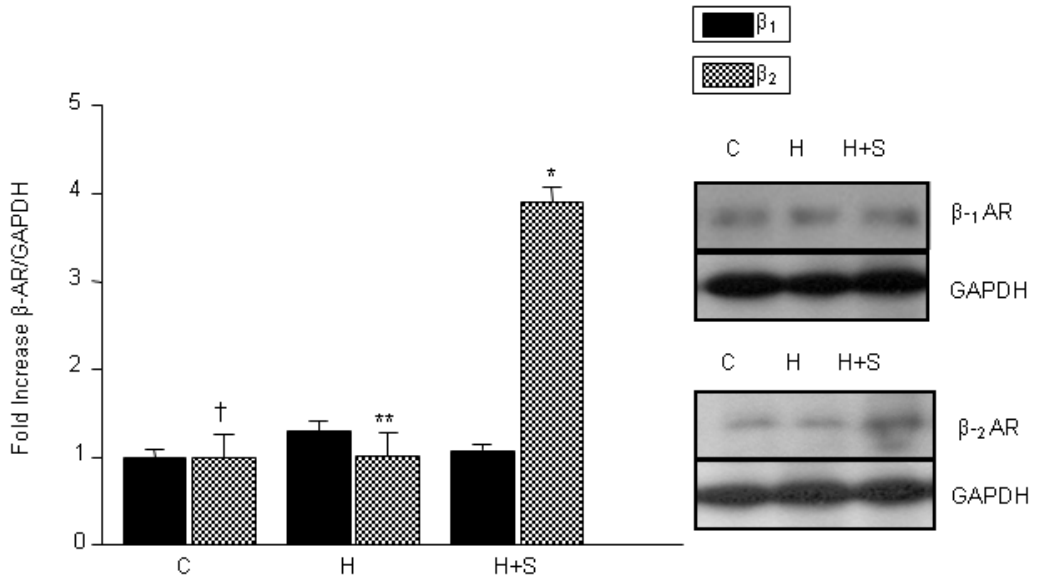
β1
β2
Fold Increase β-AR/GAPDH
5
4
3
2
1
0
†
**
*
C
H
H+S
C H H+S
β-1 AR
GAPDH
C H H+S
β-2 AR
GAPDH

Figure 3.

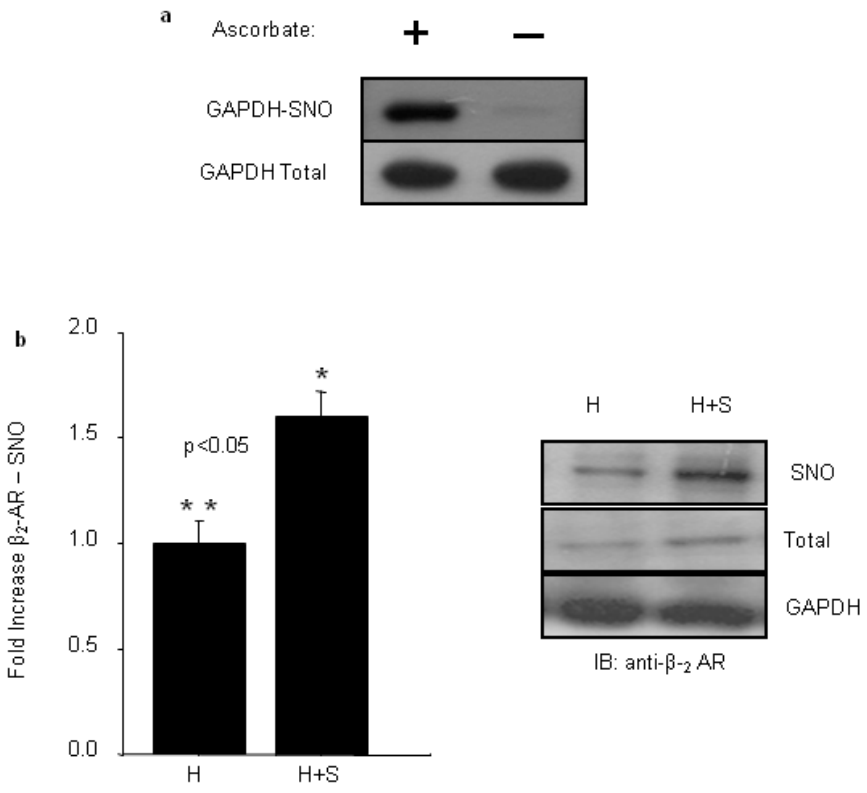
a
Ascorbate:
+
–
GAPDH-SNO
GAPDH Total
b
Fold Increase β2-AR – SNO
2.0
1.5
1.0
0.5
0.0
p<0.05
* *
*
H
H+S
H
H+S
SNO
Total
GAPDH
IB: anti-β-2 AR

Figure 4.

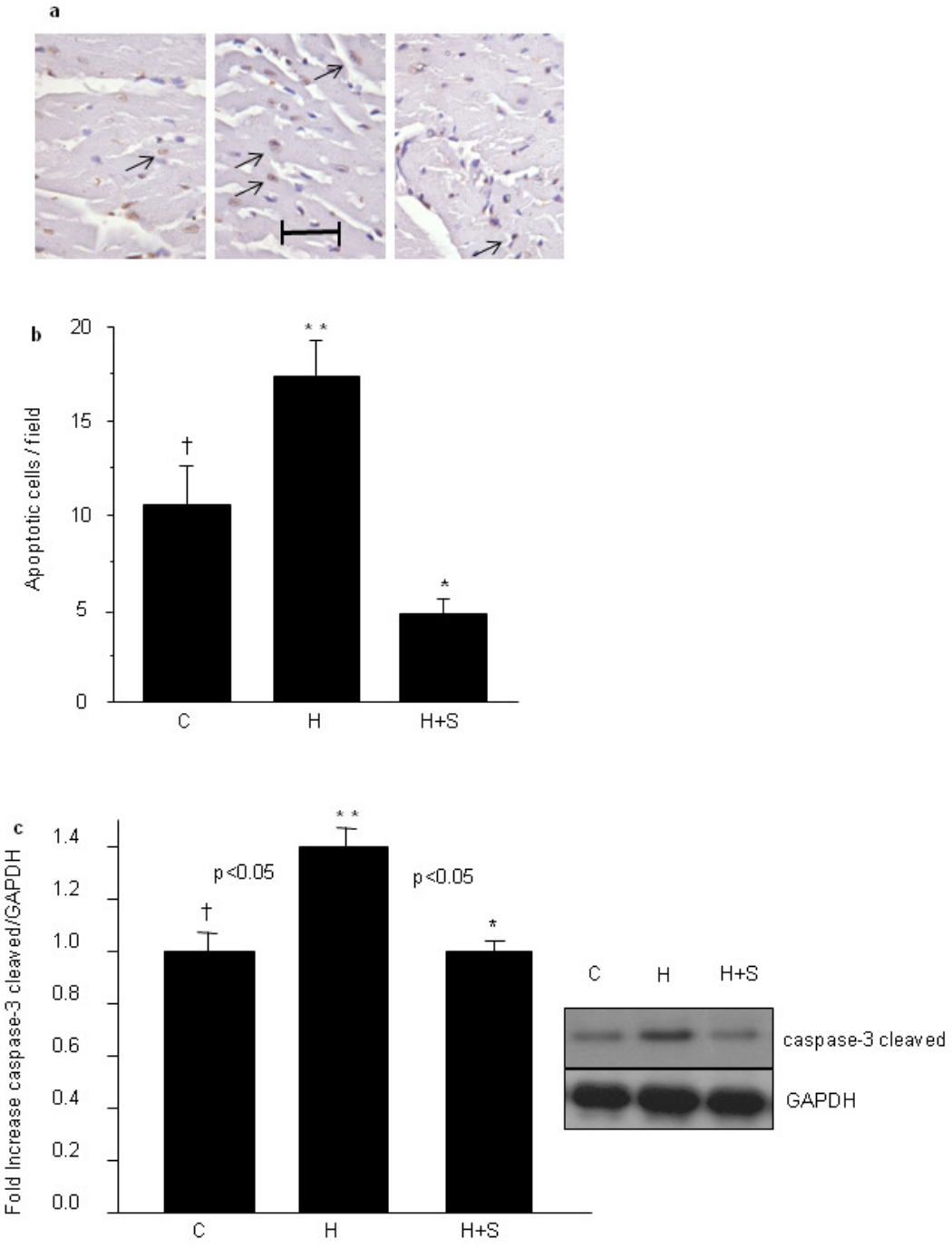
a
b
Apoptotic cells / field
20
15
10
5
0
C
H
H+S
c
Fold Increase caspase-3 cleaved/GAPDH
1.4
1.2
1.0
0.8
0.6
0.4
0.2
0.0
p<0.05
p<0.05
C
H
H+S
caspase-3 cleaved
GAPDH

Figure 5.

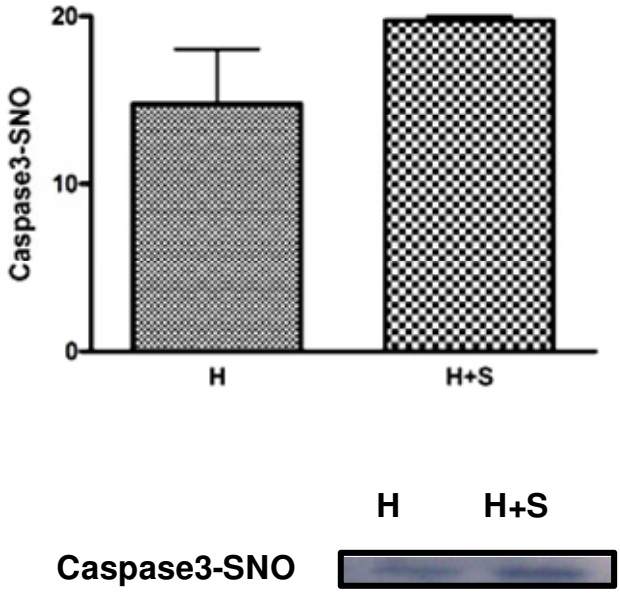

IV.2. $NO^{\bullet}$ bioavailability during early atherosclerotic development in LDLr-/- mice.

Title: $NO^{\bullet}$ bioavailability during early atherosclerotic development in LDLr-/- mice.

Amarylis Claudine Bonito Wanschel (PhD)[a], Ana Iochabel Soares Moretti (PhD)[b], Ana Carolina Tognetta Minozzi[a], Leandro dos Santos (Ms)[a], Francisco Rafael Martins Laurindo (PhD)[c], Heraldo Possolo de Souza (PhD)[b] and Marta Helena Krieger (PhD)[a,*]

[a]*Laboratory of Cardiovascular - Department of Anatomy, Cellular Biology and Physiology, State University of Campinas (UNICAMP), Biology Institute, São Paulo, Brazil;* [b]*Laboratory of Medical Investigation (LIM-51) - Department of Emergency Medicine, University of São Paulo School of Medicine (USP), São Paulo, Brazil;* [c]*Vascular Biology Laboratory - Heart Institute (InCor),School of Medicine, University of São Paulo School of Medicine (USP), São Paulo, Brazil*

***Correspondence**: **Name:** Marta Helena Krieger, PhD; **Adress:** Universidade Estadual de Campinas, Instituto de Biologia, Departamento de Anatomia, Biologia Celular e Fisiologia, 255 Monteiro Lobato Street, Laboratory 04 Campinas, SP 13083-970; **Phone:** +55 19 3521-6189; **Fax:** +55 19 3521-6185 and **email:** kriegerm@unicamp.br

ABSTRACT

Low-density lipoprotein deficient mice (LDLr-/- mice) are a useful model to study atherosclerosis, although there is little information on early disease development and atheroma installation. In this study, our goal was to evaluate the $NO^{\bullet}$ bioavailability during the different stages of atherogenesis; to accomplish this, we characterized both systemic and local biomarkers during disease progression. The systemic parameters we measured were blood pressure, lipidemic profile and atheroma size. The local parameters measured were the activity, expression and post-translational modification of the NO/NOS pathway, which is involved in the CD40/CD40L-dependent inflammatory response. The LDLr-/- mice were either fed a standard diet or high-fat diet (+ 1.25% cholesterol) from days 15 to 60. The LDLr-/- mice that were maintened on the high-fat diet showed a progressive increase in atheroma size, although this progression was not associated with a corresponding increase in the dyslipidemic profile. No changes in blood pressure were detected, although these mice are initially hypertensive. Nitrotyrosine, nNOS, iNOS and eNOS expression was not altered. However, we detected an increase in eNOS activation via phosphorylation of the eNOS at Ser1179 after 30 days on the high-fat diet. The atheroma development at 60 days blocked eNOS phosphorylation activation and the protein content of S-nitrosated. Atheromas that were induced by the high-fat diet had increased inflammation via CD40-mediated denitrosation of critical thiols by 30 and 60 days. Biomarker analysis during time course from 15 to 60 days showed that there were no changes in the systemic markers measure, although there were changes in the local parameters, such as $NO^{\bullet}$ bioavailability, inflammatory activation via denitrosation of the CD40 receptor and a reduced concentration of the total S-nitrosation protein level.

INTRODUCTION

Atherosclerosis is a complex, multifactorial disease that has both genetic and environmental determinants. Experimental studies of atherosclerosis development and progression have been greatly facilitated by the use of murine disease models, especially mice that are null for the low-density lipoprotein receptor (LDLR) gene (LDLr-/-) [1]. These LDLr-/- mice are moderately dyslipidemic, and initial reports showed that administration of a high-fat diet over 2 to 3 months causes a significant increase in the level of plasma lipids. Additionally, a high-fat diet can induce a relatively rapid development of advanced atherosclerosis, which is clinically apparent after 5 months [2-4]. Several studies have characterized these changes, although there is little information regarding the initial installation and atheroma development in this murine model.

The vascular endothelial dysfunction associated with inflammation and oxidative/nitrosative stress is an important factor that determines the prognosis of atherogenesis [5,6,], since it mediates the relationship between risk factors and the induction of an atheroma. It is well known that atherosclerotic plaque environment is under nitrosative stress [7,8], which corresponds to increase of reactive oxygen species (ROS), compounds that are formed by superoxide radical formation from a number of sources, such as the electron transport chain of mitochondria, NADPH oxidase, xanthine oxidase, uncoupled eNOS and cyclooxygenase [9].

The breakdown of the eNOS/NO pathway has been considered a major cause of vascular endothelial dysfunction [10]. The association between $NO^{\bullet}$ formation and cardiovascular disease is well known, and numerous studies have shown that $NO^{\bullet}$ exerts an anti-atherogenic effect by regulating the expression of adhesion molecules and migration of leukocytes to inflammatory sites [11,12]. Increasing evidence indicates that the

reduction in $NO^{\bullet}$ bioavailability is caused by a decrease in the expression and/or activity of eNOS and increased degradation of $NO^{\bullet}$ by reaction with superoxide [13].

$NO^{\bullet}$ modulates the inflammatory response in part by regulating the activity of the CD40/CD40L pathway [14], which plays a key role in atherosclerotic plaque development [15,16]. Therefore, the participation of $NO^{\bullet}$ on the S-nitrosation process of key proteins [17], such as those involved in the CD40-CD40L system, has been described as a signaling mechanism that is independent of cyclic guanosine monophosphate (cGMP); it is thought that this novel $NO^{\bullet}$ pathway may play a crucial role in cell signaling cascades [18,19]. The CD40 receptor has cysteine residues that are suitable substrates for S-nitrosation because they are proximal to hydrophobic environments and located between acidic and basic residues. We studied the influence of CD40 receptor S-nitrosation and the resulting signaling capability on the inflammatory process associated with atherosclerosis on the experimental LDLr-/- mouse model.

The goal of this study was to characterize both systemic and local biomarkers during early atherosclerosis development in LDLr-/- mice; the systemic biomarkers measured were the atheroma size, dyslipidemia and blood pressure, while the local parameters were the nitrosative stress level ($NO^{\bullet}$/NOS pathway and $NO_2^{\bullet-}$ $NO_3^{\bullet-}$ generation) and inflammatory activation (S-nitrosated CD-40 receptor).

MATERIALS AND METHODS

Animals

Male low-density lipoprotein receptor-deficient mice (LDLr-/-) (24 ± 3 g, n = 40) from the Jackson Laboratory (Bar Harbor, ME) were used for these experiments. The experimental protocols were approved by the Institutional Committee for Ethics in Animal Experimentation (CEEA/IB – UNICAMP), which are in agreement with the guidelines of the Brazilian Ethics Committee College for Animal Experimentation (COBEA). The mice were randomly distributed to one of six groups that were given food and water *ad libitum.* The six groups were as follows: I) control LDLr-/- mice that were fed a standard diet for 15 days (Nuvital CR1) (C15; n=6); II) hypercholesterolemic LDLr-/- mice that were fed a high-fat diet for 15 days (20% fat and 1.25% cholesterol) (H15; n=6); III) control LDLr-/- mice that were fed a standard diet for 30 days (Nuvital CR1) (C30; n=6); IV) hypercholesterolemic LDLr-/- mice that were fed a high-fat diet for 30 days (H30; n=20); V) control LDLr-/- mice that were fed a standard diet for 60 days (Nuvital CR1) (C60; n=6); and VI) hypercholesterolemic LDLr-/- mice that were fed a high-fat diet for 60 days (H60; n=8). The mice were intraperitoneally (IP) anesthetized with 6 mg/kg xylasine (Coopers, São Paulo, Brasil) and 40 mg/kg ketamine (Parke-Davis, Argentina), and the aorta was gently removed and cut into three segments. The aortic arches were used immediately for biotin-switch technique and western blotting analysis, while the other segments were used to quantify nitrite generation.

Resting blood pressure

The tail-cuff blood pressure was measured in conscious mice (between 10 a.m. and 12 a.m.) by using a computerized Kent Scientific tail–cuff system (XBP 1000). The first 6 days of measurements were for training purposes, and the data collected during these days

were not used for calculations but rather for checking measurement reproducibility. For the data used in this study, sets of 30 measurements were recorded on the specified day. On average, 20 to 30 blood pressure measurements were recorded for each mouse.

Cholesterol and triglyceride levels

Plasma from LDLr-/- mice that were fed a standard diet or high-fat diet for 15 to 60 days was obtained by centrifugation of the blood (12,000 rpm, 15 min) that was collected in heparinized tubes via the retro orbital plexus. The total cholesterol and triglyceride levels were determined with enzymatic colorimetric kits (Wako Chemicals). The results are expressed as mg/dL for six mice/group.

Histological analysis of atherosclerotic lesions in the ascending proximal aorta

Mice that were fed a high-fat diet were anesthetized, and the hearts were perfused *in situ* with phosphate-buffered saline solution (PBS), followed by 10% PBS-buffered formaldehyde. The hearts were excised and fixed in 10% formaldehyde for a minimum of 2 days. The hearts were then sequentially embedded in 5, 10 and 25% gelatin. The processing and staining was carried out according to Paigen *et al*. [20]. The lipid-stained lesions were quantified as described by Rubin *et al.* [21] with the Image Pro Plus software (version 3.0, Media Cybernetics, Silver Spring, MD). An investigator who was blinded to the treatment analyzed all of the slides. The area of the lesions was expressed as the sum of the lesions in six 10μm sections that were 80 μm distant from each other in a total aorta length of 480 μm. Because several other studies have shown that there is a predisposition for lesion development in the aortic root, this segment (extending from beyond the aortic sinus up to the point where the aorta first becomes rounded) was chosen for analysis. The results from seven mice per group are expressed in μm^2.

Western blotting código anticorpos

The frozen aorta segments of the mice were pulverized in liquid nitrogen with a mortar and pestle and resuspended in homogenization buffer comprised of 1% Triton X-100 (Amresco, Solon, Ohio), 10 mmol/l sodium pyrophosphate, 100 mmol/l sodium fluoride, 10 µg/ml Aprotinin (Amresco, Solon, Ohio), 1 mmol/l PMSF, 0.25 mmol/l sodium orthovanadate and 0.1% cocktail protease inhibitor. The samples were centrifuged for 20 min at 11,000 g, and the supernatant was collected and assayed for the total protein concentration with a Bradford kit (Bio Rad, Hercules, CA, USA). The samples were stored at −80°C until further analysis. The protein expression levels were determined via SDS-polyacrylamide gel electrophoresis under reducing conditions. The aorta tissue extract (30µg/ml) from at least four animals from each group was boiled in an equal volume of loading buffer (150 mM Tris-HCl, pH 6.8; 4% SDS; 20% glycerol; 15% β-mercaptoethanol and 0.01% bromophenol blue) and subjected to electrophoresis on 10% polyacrylamide gels. Following electrophoretic separation, the proteins were transferred to Hybond-P membranes (Amersham Pharmacia Biotech, Buckinghamshire, England). The membranes were blocked for 1 hr with 5% non-fat dry milk or bovine serum albumin (Sigma, St. Louis, MO, USA) in a buffer containing 10 mM Tris–HCl (pH 7.6), 10 mM NaCl and 0.1% Tween 20 (Calbiochem, Darmstadt, Germany) (TBST). Primary antibodies were used to quantify the following proteins: nNOS (rabbit polyclonal, 1:1000, sc648; Santa Cruz Biotechnology, Santa Cruz, CA, USA); iNOS (rabbit polyclonal, 1:1000, sc651; Santa Cruz Biotechnology, Santa Cruz, CA, USA); eNOS (rabbit polyclonal, 1:1000, sc654; Santa Cruz Biotechnology, Santa Cruz, CA, USA); eNOSpS1179 (mouse monoclonal, 1:500, 612392; BD Transduction Laboratories); CD-40 (rabbit polyclonal, 1:1000, sc9096, Santa Cruz Biotechnology, Santa Cruz, CA, USA); nitrotyrosine (mouse

monoclonal, 1:1000, 16-227 clone 1A6, Millipore) and GAPDH (rabbit polyclonal, 1:2.000, sc25778, Santa Cruz Biotechnology, Santa Cruz, CA, USA). All of the primary antibody incubations were at 4°C overnight. After the blots had been washed twice with TBST, a secondary horseradish peroxidase (HRP) conjugated antibody (goat anti-rabbit polyclonal, 1:10.000, G21234 or goat anti-mouse 81-6520, Invitrogen, Molecular Probes, Oregon, USA) was applied at a dilution of 1:10000 for 1 h. The blots were washed twice in TBST for a total of 30 min, and the immunoreactive bands were visualized with an enhanced Super Signal chemiluminescent reagent detection kit (Pierce, Rockford, IL, USA). The membranes were exposed to Kodak O-OMAT-AR photographic film (Kodak, Rochester, NY, USA), and the band intensity was quantified with Image J software.

Assessment of S-nitrosation with a chemical derivatization Biotin-switch (BST) assay coupled to immunoprecipitation and western blotting

S-nitrosated proteins in the lysate were labeled with biotin as previously described [15, 16]. The aortas were rinsed with PBS containing 0.1 mM EDTA and 0.01 mM neocuproine (Sigma, St. Louis, MO, USA), were cut into segments, and were pulverized in liquid nitrogen with a mortar and pestle. The powder was immediately resuspended in HEN lysis buffer that contained 0.1% SDS, 0.5% CHAPS and 20 mM NEM (N-ethylmaleimide) (Sigma, St. Louis, MO, USA) and lysed by rocking for 30 min at 4°C. The lysate was centrifuged for 10 min at 14,000 g at 4°C, and the NEM, which was present in excess to block sulfhydryl groups (SH), was removed by protein precipitation with acetone. The resulting pellets were resuspended in HEN buffer that contained 1% SDS (HENS). The S-nitrosothiols were reduced and biotinylated by the simultaneous addition of 10 mM sodium ascorbate as well as 0.05 mM of a sulfhydryl-specific biotinylating agent, MPB [N-(3-maleimidylpropionyl) biocytin, Molecular Probes], for 1 h at room

temperature (RT). The excess biotin was removed by a second acetone precipitation, and the proteins were resuspended in HENS buffer for subsequent immunoprecipitation of CD-40 (anti-rabbit). Biotinylation of CD-40 was detected by immunoprecipitation. The aorta tissue extract (90μg/ml) was incubated overnight in 50 μl of streptavidin–HRP. The immunoprecipitate was washed three times with 800 μL of PBS (phosphate buffered saline). Then, 20 μl of Laemmli sample buffer was added (150 mM Tris-HCl, pH 6.8; 4% SDS; 20% glycerol and 0.01% bromophenol blue) and the samples were boiled at 95°C for 5 min. Western blotting was then performed as described above. Control experiments performed in parallel did not have sodium ascorbate, thus preventing reduction of the S-nitrothiols. All of the samples were protected from light during all procedures prior to electrophoresis, and the sample densities were analyzed by the Image J software.

Nitrite generation.

The nitrite levels were measured from supernatants that were obtained from total aorta artery homogenates prepared under liquid N2. Ten-microliter aliquots were injected into a Sievers chemiluminescence analyzer (model 280) and pelleted by centrifugation with VCl3, HCl (at 95°C) and acetic acid to reduce the nitrite. The nitrite levels were normalized for total protein concentration, which was assessed with a Bradford assay.

Statistical Analyses

The results are shown as the mean ± SEM for the number of mice indicated. For multiple comparisons, the data were analyzed with ANOVA, followed by a Tukey test. For the comparison of two values, a Student's unpaired *t* test or a non-parametric Mann-Whitney test were used, as appropriate. A P-value of < 0.05 was used to indicate a statistically significant difference.

RESULTS

An increase in the lesion area is not correlated with changes in the lipid levels

The LDLr-/- mice that were fed a high-fat diet for 15, 30 and 60 days showed a progressive increase in the lesion area; there was an 87% increase in lesion area from days 15 to 30 (H15 = 92±4 *vs.* H30 = 172±8 μm^2 X 10^3, n=7; $P<0.05$) and a 53% increase from days 30 to 60 (H30 *vs.* H60 = 263±50 μm^2 X 10^3, n=7; $P<0.05$), as is shown in Figure 1.

The plasma cholesterol and triglyceride (TG) concentrations are shown in Table I; there was no significant change in the plasma cholesterol and triacylglycerol levels over time (ANOVA, *P*=NS). Compared to the LDLr-/- mice that were fed a standard diet, the LDLr-/- that were fed a high-fat diet for 15, 30 and 60 days had a increase in their plasma cholesterol concentration. The following values were obtained for cholesterol concentration measurements from each group of LDL-/- mice: H15 = 820 ±101 *vs.* C15 = 251 ±17 mg/dl (after 15 days, n = 6; $P<0.001$); H30 = 957 ±81 *vs.* C30 = 303 ±18 (after 30 days, n = 6; $P<0.001$); and H60 = 949 ±85 *vs.* C60 = 281 ±15 (after 60 days, n = 6; $P<0.001$).

There was a significant difference in the plasma cholesterol level between the mice fed low and high-cholesterol diets; there were smaller, non-significant differences between treatment times of the mice that were fed the same diet. The triglyceride (TG) concentration was similar among all of the experimental groups (Table I).

The blood pressure did not change with atheroma development

The effect of atheroma development on blood pressure in LDLr-/- mice that were fed a high-fat or standard diet was assessed by a tail-cuff measurement. The resting systolic pressure in the LDLr-/- mice that were fed a high-fat diet for 15, 30 and 60 days did not differ among the experimental groups (H15 = 143 ± 3 mm Hg, *n* = 6; H30 = 145 ±

9 mm Hg, *n* = 6 and H60 = 141 ± 2 mm Hg, *n* = 6) or the control groups (C15 = 141 ± 3 mm Hg, *n* = *6*; C30 = 142 ± 3 mm Hg, *n* = *6* and C60 = 144 ± 2 mm Hg, *n* = *6*) (Figure 2) (ANOVA, *P*=NS).

A change in NO and eNOS activation is associated with atheroma development

Analysis of aortic total eNOS, nNOS and iNOS protein expression levels showed that the expression level of these proteins did not change among LDLr-/- mice that were fed a high-fat diet or standard diet for 15, 30 and 60 days (Figure 3A, B and C).

The LDLr-/- mice that were fed a standard diet for 15, 30 and 60 days had changes in the phosphorylation of eNOS at Ser-1179 (p-eNOS). The p-eNOS level was 119% higher by day 30, compared to day 15 (1.16 ± 0.08, n= 4 *vs.* 0.53± 0.08, n = 4; *P*<0.05); after 60 days, the level returned to the day 15 baseline (C60, 0.60 ±0.1, n = 4; *P*<0.05) (Figure 4A).

The LDLr-/- mice that were fed a high-fat diet for 15, 30 and 60 days had changes in the amount of p-eNOS. Compared to the 15-day group that was fed a high-fat diet, the 30-day group had a 46% increase in the level of p-eNOS (1.20 ± 0.1, n = 4 *vs.* 1.74 ± 0.07, n = 4, respectively; *P*<0.05); these data suggest that acute atherosclerosis increases the ratio of p-eNOS/eNOS. This increase in p-eNOS was partially blocked after 60 days of a high-fat diet (0.95 ± 0.05, n = 4; *P*<0.01) (Figure 4A).

Compared to the LDLr-/- mice that were fed a standard diet, by days 15 and 30 the LDLr-/- high-fat diet mice had a higher level of p-eNOS (C15, 0.53± 0.08 *vs.* H15, 1.20 ± 0.1; *P*<0.01 and C30, 1.16 ± 0.08 *vs.* H30, 1.74 ± 0.07; P<0.05). However, the p-eNOS level at 60 days was not significantly different between the groups, as is shown in Figure 4B.

The *S*-nitrosated protein concentration was significantly reduced in the aorta from LDLr-/- mice that were fed a standard diet for 60 days, compared to the 15- and 30-day fed mice (C60 = 0.22 ± 0.06 *vs.* C15 = 0.56 ± 0.05; $P<0.01$ and *vs.* C30 = 0.67 ± 0.04; $P<0.01$). LDLr-/- mice that were fed a high-fat diet for 60 days had a similar decrease in the concentration of *S*-nitrosated proteins (H60 = 0.2 ± 0.05 *vs.* H15 = 0.74 ± 0.1; $P<0.001$ and *vs.* H30 = 0.53 ± 0.03; $P<0.05$) (Figure 5).

Nitrosative stress was not detected during atheroma development

Nitrotyrosine (NT) is often used as a biomarker for the formation of reactive nitrogen species, specifically peroxynitrite-induced protein modification. There was no difference in the aortic NT level among the various groups we tested (Figure 6).

The inflammatory response increased with atheroma development

Because any $NO^{\bullet}$ produced *in vivo* is further metabolized to nitrite, we measured the nitrite levels to approximate the amount of $NO^{\bullet}$ production. There was an increase in nitrite production in the aorta tissue in LDLr-/- mice that were fed a standard diet for 15 and 30 days (C15 = 0.92 ± 0.2 *vs.* C30 = 4.5 ± 0.9; $P<0.001$) and from 15 to 60 days (C15 = 0.92±0.2 *vs.* C60 = 5.1 ± 1; $P<0.01$). However, significantly lower values were obtained from LDLr-/- mice that were fed a high-fat diet compared to a standard diet for 30 and 60 days (C30 = 4.5 ± 0.9 *vs.* H30 = 1.6 ± 0.5; $P<0.001$ and C60 = 5.1 ± 1 *vs.* H60 = 1.5 ± 0.6; $P<0.001$) (Figure 7A).

CD40 nitrosation was measured after 15, 30 and 60 days with the biotin switch method. The S-nitrosated protein level was reduced in LDLr-/- mice that were fed a high-fat diet compared to mice fed a standard diet for 30 and 60 days (Fig 7B).

DISCUSSION

The present study shows that LDLr-/- mice that were fed a high-fat diet for 15, 30 and 60 days exhibit a progressive increase in the lesion area and that this increase does not correlate with changes in the cholesterol and triglyceride level. In this study, we determinated local changes during the initial phase of atherogenesis, such as vascular bioavailability of nitric oxide and inflammatory activation via S-nitrosation, during a time-course study of 60 days. However, no systemic changes, such as changes in blood pressure or the dyslipidemia value, were detected.

LDLr-/- mice that were fed a standard diet showed a spontaneous development of atherosclerotic lesions during 15 days, although these lesions developed were relatively moderate and 50% smaller than lesions seen with a high-fat diet during the same period. The cholesterol levels from LDLr-/- mice were 250 mg/dl (standard diet) and 820 mg/dl (high-fat diet). These results indicate that the LDL receptor knockout mice are dyslipidemic and develop atheromas independently from their diet. This phenomenon has been described in other studies [22,23] which histological examination of the aortic roots from mice that were fed a standard diet for 12 months showed that there were small accumulations of intimal foam cells within the walls of the coronary sinuses. Further analysis showed that these mild pathological manifestations were associated with a two-fold increase in the plasma cholesterol level [24,22]. However, severe lesions were observed when the mice were fed an atherogenic diet [25]. Time-course analysis of LDLr-/- mice that were fed a high-fat diet for 15, 30 and 60 days showed that there was a 50%, 37% and 53% increase in the number of atherosclerotic lesions, respectively. However, this increase was not associated with a change in the dyslipidemic profile. This increase in lesion area is independent from the lipidemic profile and may be caused by additional risk

factors, such as an increase in superoxide production, apoptosis, vasoconstriction and/or endothelial dysfunction. However, LDLr-/- mice that were fed a high-fat diet for longer than 60 days had a significantly elevated average plasma cholesterol level [1,22].

Previous studies from our laboratory [26,27] have shown that male LDLr/- mice fed a standard diet (C) have a hypertensive phenotype compared to their wild-type C57Bl7 counterparts (130 ± 2 *vs.* 141 ± 3 mmHg; systolic blood pressure). In the present study, there was no change in the blood pressure values from LDLr-/- mice that were fed a high-fat diet for 15, 30 or 60 days. However, these values are hypertensive when compared to the wild-type C57Bl7 counterparts. Hypertension in male LDLr-/- mice has been attributed to deletion of the LDL receptor gene, and a high-fat diet does not seem to further increase the blood pressure [26]. In the present study, the time-course analysis showed that there was a progressive increase in atheroma development from days 15, 30 and 60 in LDLr -/- mice that were fed a high-fat diet, although this effect was independent of the hypertensive phenotype. “However, clinical studies have shown that hypertension is associated with an increase in atherosclerotic plaque development. Yang and colleagues [28] have suggested that chronic atherosclerosis in a mouse model, such as the apolipoprotein E knockout mice, results in hypertension and endothelial dysfunction similar to what is seen in the advanced human disease”. In summary, our analysis of systemic biomarkers showed that there was only a change in the size of the atheroma over time, not in the blood pressure or plasma lipid levels.

In relation to local biomarkers on the temporal course of the atherogenic response, the production of NO• plays an essential role in vascular protection. This increased activation of eNOS (via phosphorylation of residue at Ser-1179) in the aorta of LDLr-/- mice that were fed a high-fat diet from 15 to 30 days may be an emergency mechanism to

produce this protein isoform. This increase in eNOS activation could be due to a negative feedback control that was stimulated by a decrease in the bioavailability of $NO^{\bullet}$, which may result from increased production of oxygen free radicals in the aorta of these animals at 15 days [29]. However, this increase in eNOS activation was not maintained, and there was a decrease in p-eNOS during days 30 to 60 with the high-fat diet. It is well known that shear stress increases eNOS activity, and studies "*in vivo*" have shown that the anatomical sites where atheromas develop are associated with a decrease in eNOS activity. It has also been shown that a decrease in eNOS phosphorylation is associated with enhanced susceptibility to atherosclerosis [30,31]. In cultured endothelial cells that were stimulated with increasing shear stress, eNOS was rapidly phosphorylated [32,33]. Although many signal-transducing molecule can phosphorylate eNOS, AKT1 has been predominantly studied. ApoE-/-Akt1-/- (serine/threonine kinase Akt) mice develop severe atherosclerosis, have an inflamed arterial wall, increased macrophage infiltration and have a marked decrease in p-eNOS (but not the total eNOS level) [34,35].

Alterations in the level of p-eNOS, as well as the total S-nitrosation protein level, were similar between the mice on a standard or high-fat diet over the time-course. We hypothesized that this pattern may result from natural atherosclerosis vasculature aging, which was observed in studies that associated eNOS activation with aging more advanced [36,37].

In the present study, the S-nitrosation of the CD40 receptor represents a local biomarker for the inflammatory activation process. The CD40/CD40L system plays a key role in atherosclerotic plaque formation [15,16], and in vivo studies with hyperlipidemic mice have confirmed the role of CD40-receptor signaling during atherogenesis. Atheroma development in LDLr -/- mice that were fed a high-fat diet for 30 or 60 days had a decrease

in the level of S-nitrosated CD40-receptor. It has been previously shown that inflammatory activity is increased with denitrosation of CD40-receptor [14], which participates in atherosclerosis [15]; thus, we used CD40-receptor as an inflammatory marker in our present study. The decrease in S-nitrosated CD40-receptor that we observed may be correlated to reduced levels of nitrite, which was used as an indicator of $NO^{\bullet}$ production. However, this reduction in $NO^{\bullet}$ bioavailability and the consequential increase in CD40-receptor denitrosation (that causes inflammation) were not observed during analysis of nitrotyrosine.

Our results show that after 60 days there were changes in local, but not systemic, biomarkers. However, future studies are needed to verify that additional systemic biomarkers are not altered.

REFERENCES

1. Ishibashi S, Brown MS, Goldstein JL, Gerard RD, Hammer RE, Herz J (1993) Hypercholesterolemia in low density lipoprotein receptor knockout mice and its reversal by adenovirus-mediated gene delivery. J Clin Invest 92:883– 893

2. Smithies O, Maeda N (1995) Gene targeting approaches to complex genetic diseases: atherosclerosis and essential hypertension. Proc Natl Acad Sci U S A 92:5266 –5672

3. Plump A (1997) Atherosclerosis and the mouse: a decade of experience. Ann Med 29:193–198

4. Breslow JL (1996) Mouse models of atherosclerosis. Science 272:685–688

5. Hulsmans M, Holvoet P (2010) The vicious circle between oxidative stress and inflammation in atherosclerosis. J Cell Mol Med 14:70-8

6. Landmesser U, Hornig B, Drexler H (2004) Endothelial function: a critical determinant in atherosclerosis? Circulation 109:II27-33

7. Vogiatzi G, Tousoulis D, Stefanadis CH (2009) The role of oxidative stress in atherosclerosis. J Cardiol 50:402-9

8. Stocker R. Keaney JF Jr (2004) Role of oxidative modifications in atherosclerosis. Physiol. Rev 84:1381–1478

9. Landmesser U, Spiekermann S, Dikalov S, Tatge H, Wilke R, Kohler C, Harrison DG, Horning B, Drexler H (2002) Vascular oxidative stress and endothelial dysfunction in patients with chronic heart failure: role of xanthine-oxidase and extracellular superoxide dismutase. Circulation 106:3073–8

10. Huang PL (2003) Endothelial nitric oxide synthase and endothelial dysfunction. Curr Hypertens Rep 5:473-80

11. Madamanchi NR, Vendrov A, Runge MS (2005) Oxidative stress and vascular disease. Arterioscler Thromb Vasc Biol 25:29–38

12. Stokes KY, Cooper D, Tailor A, Granger DN (2002) Hypercholesterolemia promotes inflammation and microvascular dysfunction: role of nitric oxide and superoxide. Free Radic Biol Med 33:1026–1036

13. Pepine CJ (2009) The impact of nitric oxide in cardiovascular medicine: untapped potential utility. Am J Med 122:S10-5

14. Godoy LC, Moretti AI, Jurado MC, Oxer D, Janiszewski M, Ckless K, Laurindo FR, Souza HP (2009) Loss of CD40 Endogenous S-Nitrosylation During Inflammatory Response in Endotoxemic Mice and Septic Patients. Shock

15. Mach F, Schoenbeck U, Sukhova G, Atkinson E, Libby P (1998) Reduction of atherosclerosis in mice by inhibition of CD40 signaling. Nature 394:200–3

16. Schönbeck U, Libby P (2001) CD40 signaling and plaque instability. Circ Res 89:1092-103

17. Stamler JS, Toone EJ, Lipton SA, Sucher NJ (1997) (S)NO signals: translocation, regulation, and a consensus motif. Neuron 18:691-6

18. Mach F, Schönbeck U, Libby P (1998) CD40 signaling in vascular cells: a key role in atherosclerosis? Atherosclerosis 137:S89-95

19. Cattaruzza M, Słodowski W, Stojakovic M, Krzesz R, Hecker M (2003) Interleukin-10 induction of nitric-oxide synthase expression attenuates CD40-mediated interleukin-12 synthesis in human endothelial cells. J Biol Chem 278:37874-80

20. Paigen B, Morrow A, Holmes PA, Mitchell D, Williams RA (1987) Quantitative assessment of atherosclerotic lesions in mice. Atherosclerosis 68:231-40

21. Rubin E, Krauss R, Spangler E, Verstuyft J, Clift S (1991) Inhibition of early atherogenesis in transgenic mice by human apolipoprotein AI. Nature 353:265-7

22. Ishibashi S, Goldstein JL, Brown MS, Herz J, Burns DK (1994) Massive xanthomatosis and atherosclerosis in cholesterol-fed low density lipoprotein receptor-negative mice. J Clin Invest 93:1885-93

23. Yoshimatsu M, Terasaki Y, Sakashita N, Kiyota E, Sato H, van der Laan LJ, Takeya M (2004) Induction of macrophage scavenger receptor MARCO in nonalcoholic steatohepatitis indicates possible involvement of endotoxin in its pathogenic process. Int J Exp Pathol 85:335-43

24. Moore RE, Kawashiri MA, Kitajima K, Secreto A, Millar JS, Pratico D, Rader DJ (2003) Apolipoprotein A-I deficiency results in markedly increased atherosclerosis in mice lacking the LDL receptor. Arterioscler Thromb Vasc Biol 23:1914-20

25. Lichtman AH, Clinton SK, Iiyama K, Connelly PW, Libby P, Cybulsky MI (1999) Hyperlipidemia and atherosclerotic lesion development in LDL receptor- deficient mice fed defined semipurified diets with and without cholate. Arterioscler Thromb Vasc Biol 19:1938-44

26. Garcia JA, dos Santos L, Moura AL, Ricardo KF, Wanschel AC, Shishido SM, Spadari-Bratfisch RC, de Souza HP, Krieger MH (2008) S-nitroso-N-acetylcysteine (SNAC) prevents myocardial alterations in hypercholesterolemic LDL receptor knockout mice by antiinflammatory action. J Cardiovasc Pharmacol 51:78-85

27. Trieu VN, Uckun FM (1998) Male-associated hypertension in LDL-R deficient mice. Biochem Biophys Res Commun 247:277-9

28. Yang R, Powell-Braxton L, Ogaoawara AK, Dybdal N, Bunting S, Ohneda O, Jin H (1999) Hypertension and endothelial dysfunction in apolipoprotein E knockout mice. Arterioscler Thromb Vasc Biol 19:2762-8

29. Krieger MH, Santos KFR, Shishido SM, Wanschel AC, Estrela HF, Santos L, De Oliveira MG, Franchini KG, Spadari-Bratfisch RC, Laurindo FR (2006) Antiatherogenic effects of S-nitroso-N-acetylcysteine in hypercholesterolemic LDL receptor knockout mice. Nitric Oxide 14:12–20

30. Imrie H, Abbas A, Viswambharan H, Rajwani A, Cubbon RM, Gage M, Kahn M, Ezzat VA, Duncan ER, Grant PJ, Ajjan R, Wheatcroft SB, Kearney MT (2009) Vascular Insulin-Like Growth Factor-I Resistance and Diet-Induced Obesity. Endocrinology 150:4575–4582

31. Wong WT, Ng CH, Tsang SY, Huang Y, Chen ZY (2009) Relative contribution of individual oxidized components in ox-LDL to inhibition on endothelium-dependent relaxation in rat aorta. Nutrition, Metabolism & Cardiovascular Diseases 1-8.

32. Dimmeler S, Fleming I, Fisslthaler B, Hermann C, Busse R, Zeiher AM (1999) Activation of nitric oxide synthase in endothelial cells by Akt-dependent phosphorylation. Nature 399:601–605

33. Gallis B, Corthals GL, Goodlett DR, Ueba H, Kim F, Presnell SR, Figeys D, Harrison DG, Berk BC, Aebersold R, Corson MA (1999) Identification of flow-dependent endothelial nitric oxide synthase phosphorylation sites by mass spectrometry and regulation of phosphorylation and nitric oxide production by the phosphatidylinositol 3-kinase inhibitor LY294002. J Biol Chem 274:30101–30108

34. Fernández-Hernando C, József L, Jenkins D, Di Lorenzo A, Sessa WC (2009) Absence of Akt1 reduces vascular smooth muscle cell migration and survival and induces features

of plaque vulnerability and cardiac dysfunction during atherosclerosis. Arterioscler Thromb Vasc Biol 29:2033-40

35. Fernández-Hernando C, Ackah E, Yu J, Suárez Y, Murata T, Iwakiri Y, Prendergast J, Miao RQ, Birnbaum MJ, Sessa WC (2007) Loss of Akt1 leads to severe atherosclerosis and occlusive coronary artery disease. Cell Metab 6:446-57

36. Hoffmann J, Haendeler J, Aicher A, Rössig L, Vasa M, Zeiher AM, Dimmeler S (2001) Important Role of Nitric Oxide Aging Enhances the Sensitivity of Endothelial Cells Toward Apoptotic Stimuli Circ Res 89:709-715

37. Wilcox JN, Subramanian RR, Sundell CL, Tracey WR, Pollock JS, Harrison DG, Marsden PA (1997) Expression of multiple isoforms of nitric oxide synthase in normal and atherosclerotic vessels. Arterioscler Thromb Vasc Biol 17:2479 –2488

FIGURE LEGENDS

Figure 1. Atheroma Development. The development of an atheroma in the aortic root of LDL-/- male mice that were fed a high-fat diet for 15, 30 and 60 days is shown. All of the data represent the mean ± SEM; n = 7 mice for each group. Atheroma formation was significantly increased in mice that were fed a high-fat diet at 30 days compared to 15 days (H30 = 172 ± 8 *vs.* H15 = 92 ± 4 μm^2 X 10^3, n=7; $P<0.05$*) and at 60 days compared to 30 days (H60 = 263 ± 50 *vs.* H30 = 172 ± 8 μm^2 X 10^3, n=7; $P<0.05$**).

Figure 2. Systolic blood pressure. The tail-cuff blood pressure was measured in conscious mice with a computerized tail-cuff Kent Scientific (XBP 1000) system. The values shown are the mean ± SEM for at least six animals from each group (ANOVA, *P*=NS).

Figure 3. The nNOS, iNOS and eNOS protein expression levels in the aorta. Mice aorta proteins (30 µg) were separated on a SDS 12% polyacrylamide gel and examined by Western blot analysis with a polyclonal antibody against nNOS, iNOS, eNOS and GAPDH; n = 4 animals per group. The mice were euthanized, and the aorta tissue was lysed and centrifuged. Thirty micrograms of protein was separated by SDS-polyacrylamide gel electrophoresis and transferred to a nitrocellulose membrane. The proteins were quantified by densitometry, normalized to the GAPDH protein expression level, and are expressed as the percentage of change (%C15). The values are means ± SEM, which was calculated from at least four animals from each group (ANOVA, *P*=NS).

Figure 4. The relative protein expression level of S1179 p-eNOS and eNOS. The aortic tissue was lysed and centrifuged, and 30 µg of protein was separated by SDS-polyacrylamide gel electrophoresis and transferred to a nitrocellulose membrane; the membranes were probed with antibodies against phosphorylated or unphosphorylated endothelial nitric oxide synthase (eNOSpSer1177 and eNOS). The proteins were quantified

by densitometry, and the phosphorylated protein level was normalized to either the unphosphorylated protein and GAPDH expression level; the data are expressed as the percentage of change relative to the control mice (%C15) (A) $^{\dagger}P<0.05$ compared to the C15 mice, $^{\dagger\,\dagger}P<0.05$ compared H15 mice, $^{*}P< 0.05$ compared C30 mice and $^{**}P< 0.05$ compared to H30 mice; (B) $^{\dagger}P<0.01$ compared to C15 mice and $^{*}P<0.05$ compared to C30 mice (ANOVA+ Tukey test).

Figure 5. Quantification of the S-nitrosated protein content of aortic tissue with the Biotin Switch (BST) method. The aortic tissue was subjected to the BST labeling, the biotinylation reaction (30 µg), and was analyzed by immunoblotting. GAPDH were shown to indicate equal amount of proteins loaded. The data are the mean ± SEM (n=4). C15, C30, and C60 represent LDLr-/- mice that were fed a standard diet for 15, 30 and 60 days, respectively; H15, H30 and H60 represent LDLr-/- mice that were fed a high-fat diet for 15, 30 and 60 days, respectively. The same letters indicate pairwise comparisons that are significantly different (ANOVA+ Tukey test). $^{a,d}P<0.001$, $^{b}P<0.05$ and $^{C}P<0.01$.

Figure 6. Nitrotyrosine protein expression in the aorta. Mice aorta (30 µg proteins) were separated on a SDS 10% polyacrylamide gel and examined by Western blot analysis using a polyclonal antibody against nitrotyrosine. The data are presented as the mean ± SD, n = 4 (ANOVA, *P*=NS).

Figure 7. S-nitrosation of the CD40 receptor and Nitrite production levels in the aorta. (A) The aortic tissue was subjected to the BST and biotinylation reactions, and an aliquot (~100 µg) of the whole tissue lysate was analyzed by immunoblotting with avidin–HRP and an anti-CD40 antibody (for input). $^{*}P<0.001$ *vs.* C30 and $^{**}P<0.001$ *vs.* C60. (B) The nitrite levels in the aorta after treatment. The total protein concentration was normalized

with a Bradford assay. The same letters indicate pairwise comparisons that are significantly different. [a,b,c,d] $P<0.001$, student's *t*-test.

	CHOL	TG
C15	251 ± 17[a]	139 ± 12
H15	820 ± 101[a]	175 ± 26
C30	303 ± 18[b]	132 ± 8.7
H30	957 ± 81[b]	173 ± 26
C60	281 ± 15[c]	148 ± 21
H60	949 ± 85[c]	155 ± 20

Table1. Abreviations CHOL, cholesterol; TG, triglyceride. Values represent mean±s.e.m. (n=6). The same letters indicate the pair comparisons that are significantly different. [a,b,c] $P<0.001$, Student *t*-test.

Figure 1.

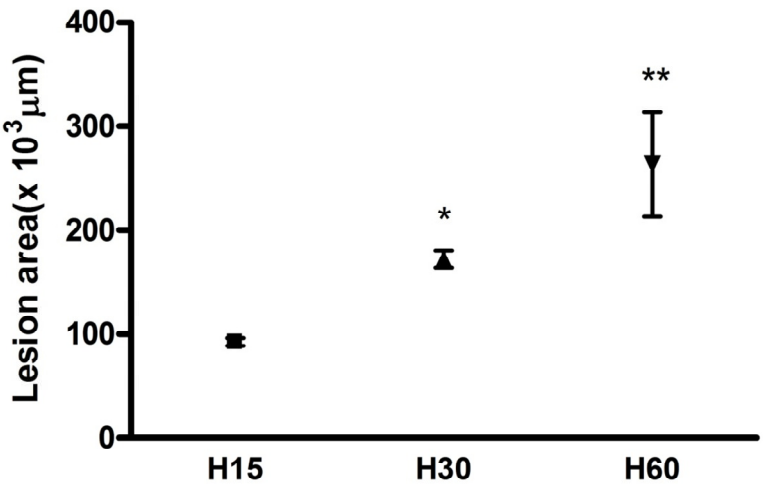

Figure 2.

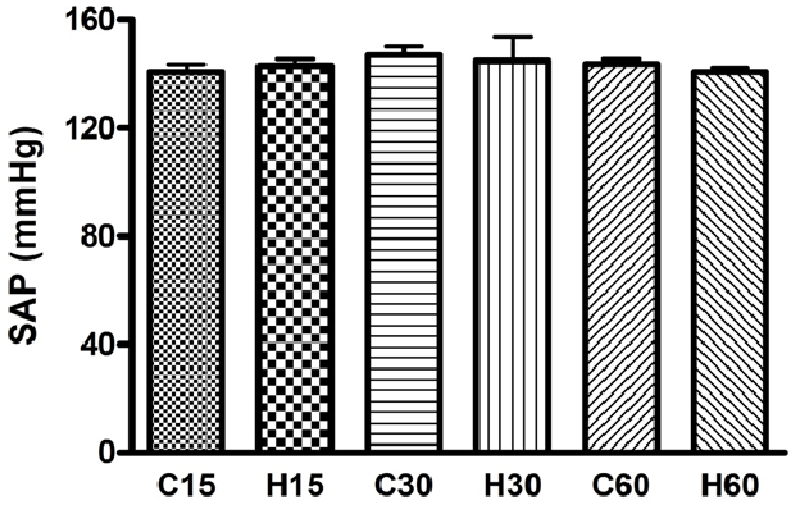

Figure 3A.

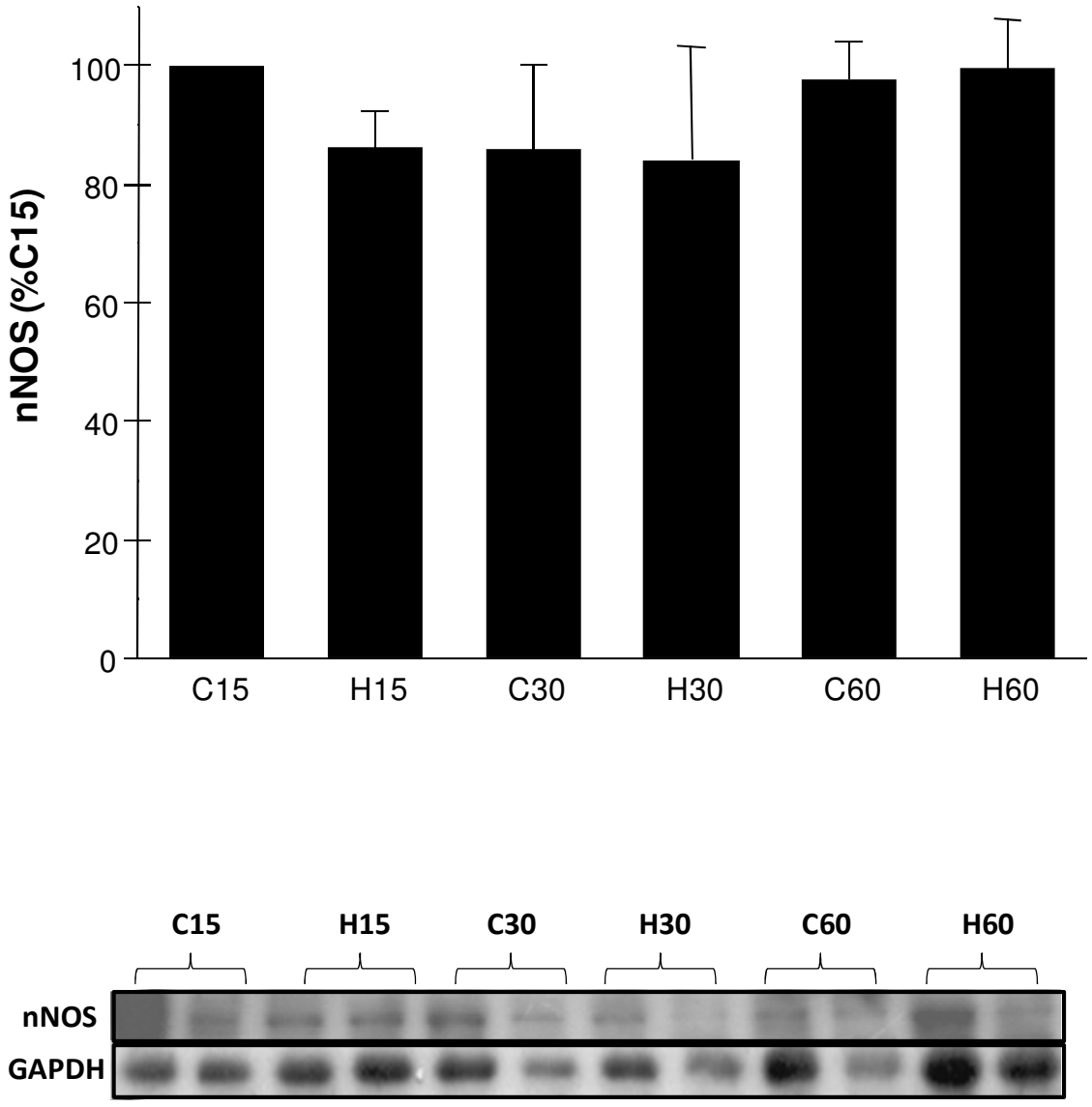
nNOS (%C15)
100
80
60
40
20
0
C15
H15
C30
H30
C60
H60
C15
H15
C30
H30
C60
H60
nNOS
GAPDH

Figure 3B.

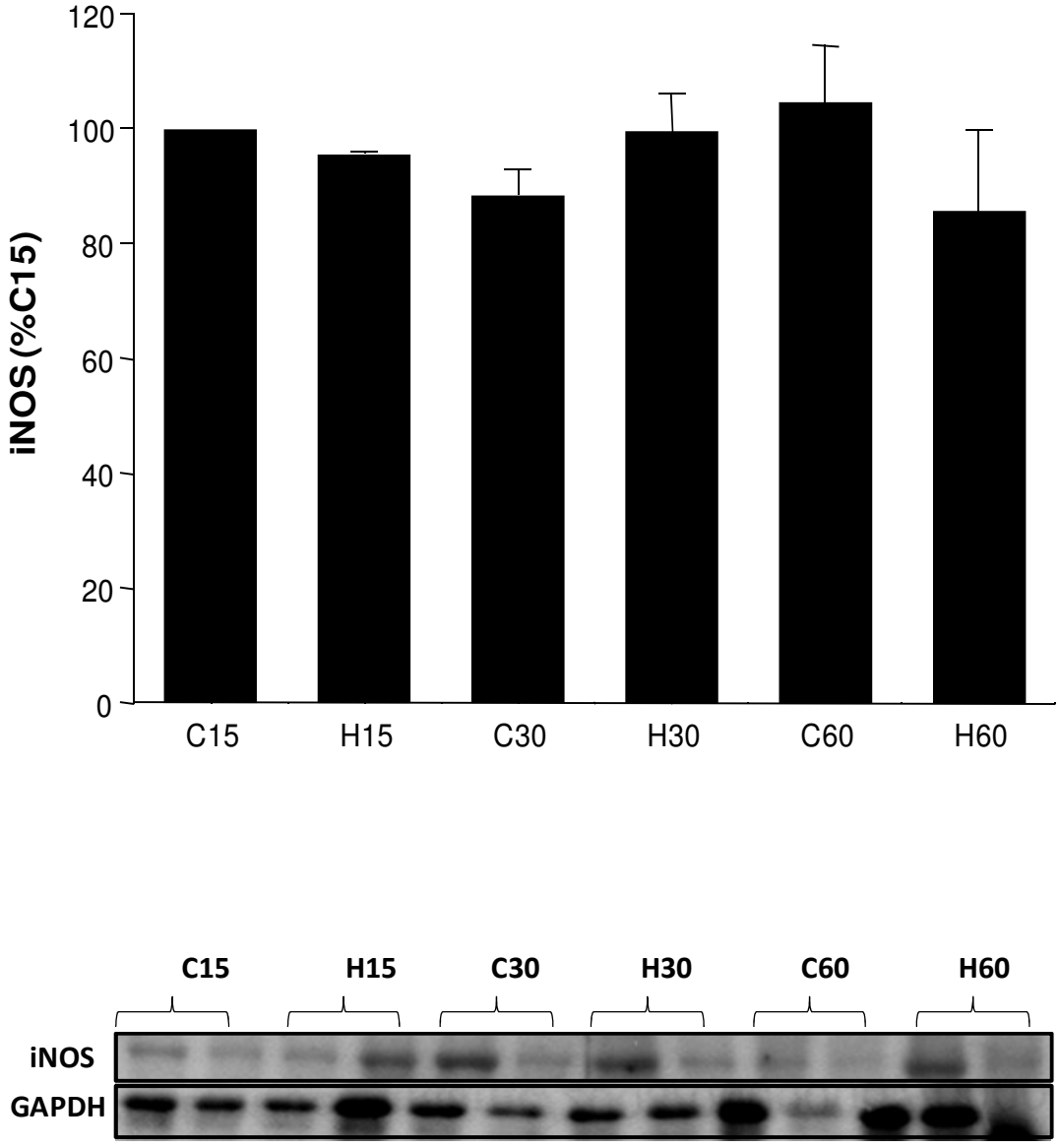
120
100
80
60
40
20
0
iNOS (%C15)
C15
H15
C30
H30
C60
H60
C15
H15
C30
H30
C60
H60
iNOS
GAPDH

Figure 3C.

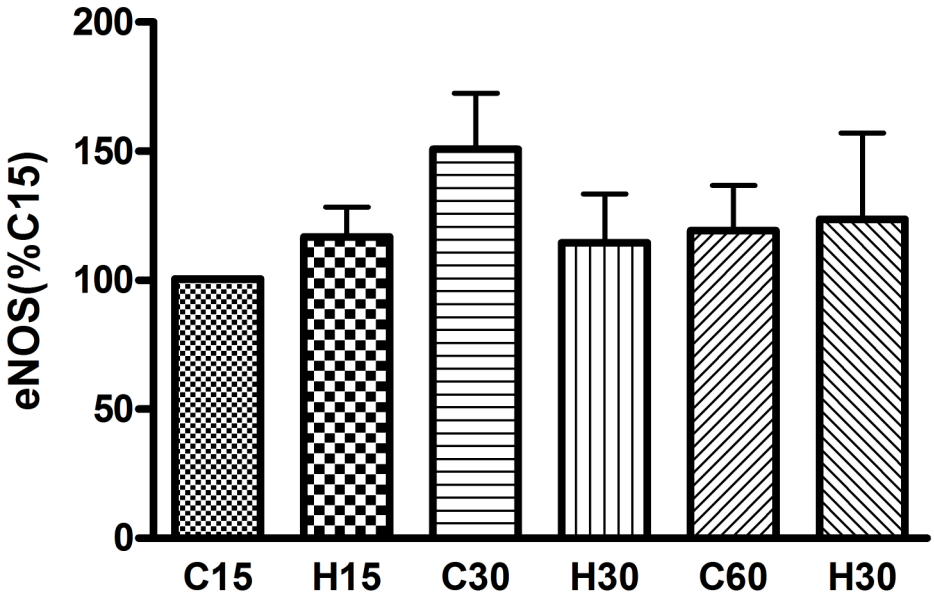
200
150
100
50
0
eNOS(%C15)
C15
H15
C30
H30
C60
H30

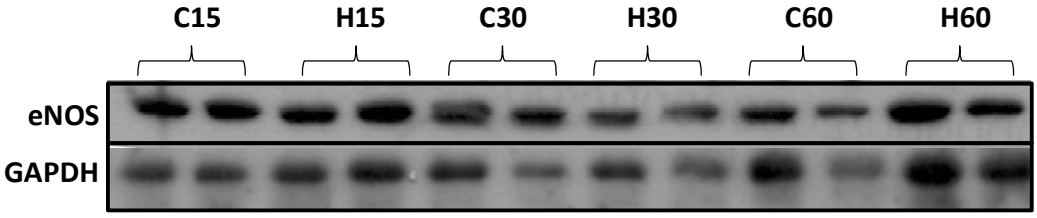
C15
H15
C30
H30
C60
H60
eNOS
GAPDH

.

Figure 4A.

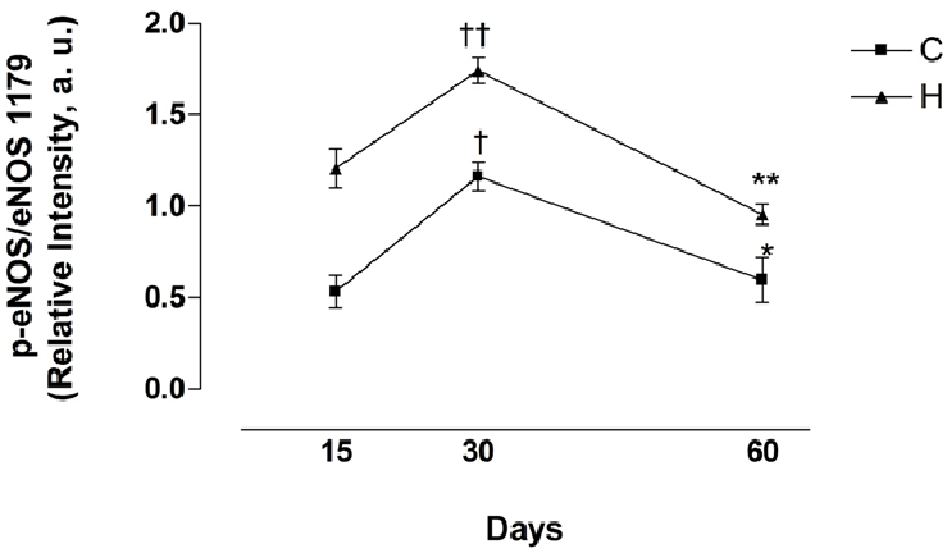

Figure 4B.

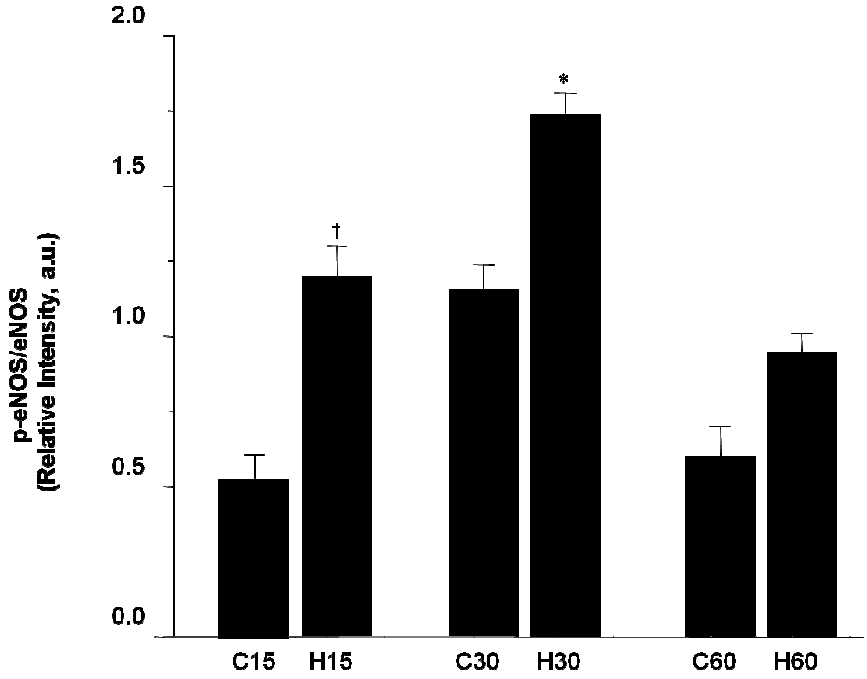

Figure 5.

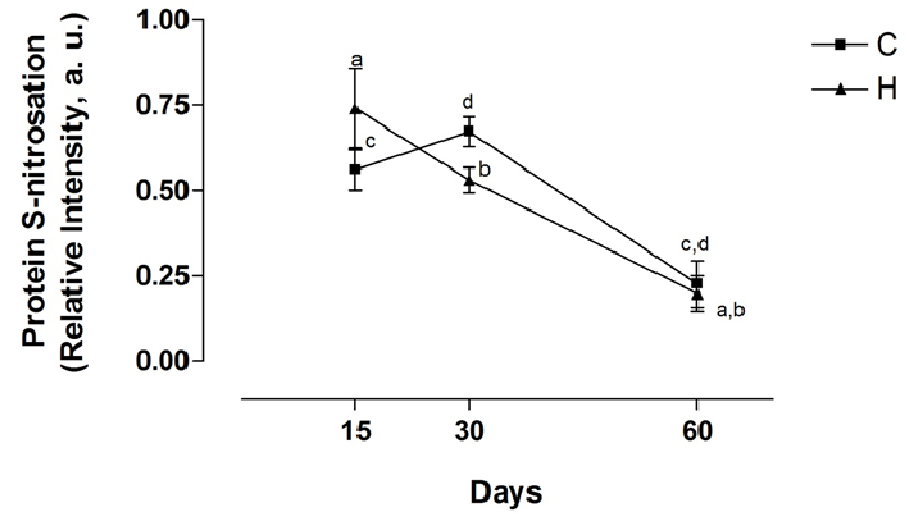
Protein S-nitrosation
(Relative Intensity, a. u.)
1.00
0.75
0.50
0.25
0.00
a
c
d
b
c,d
a,b
15
30
60
Days
C
H

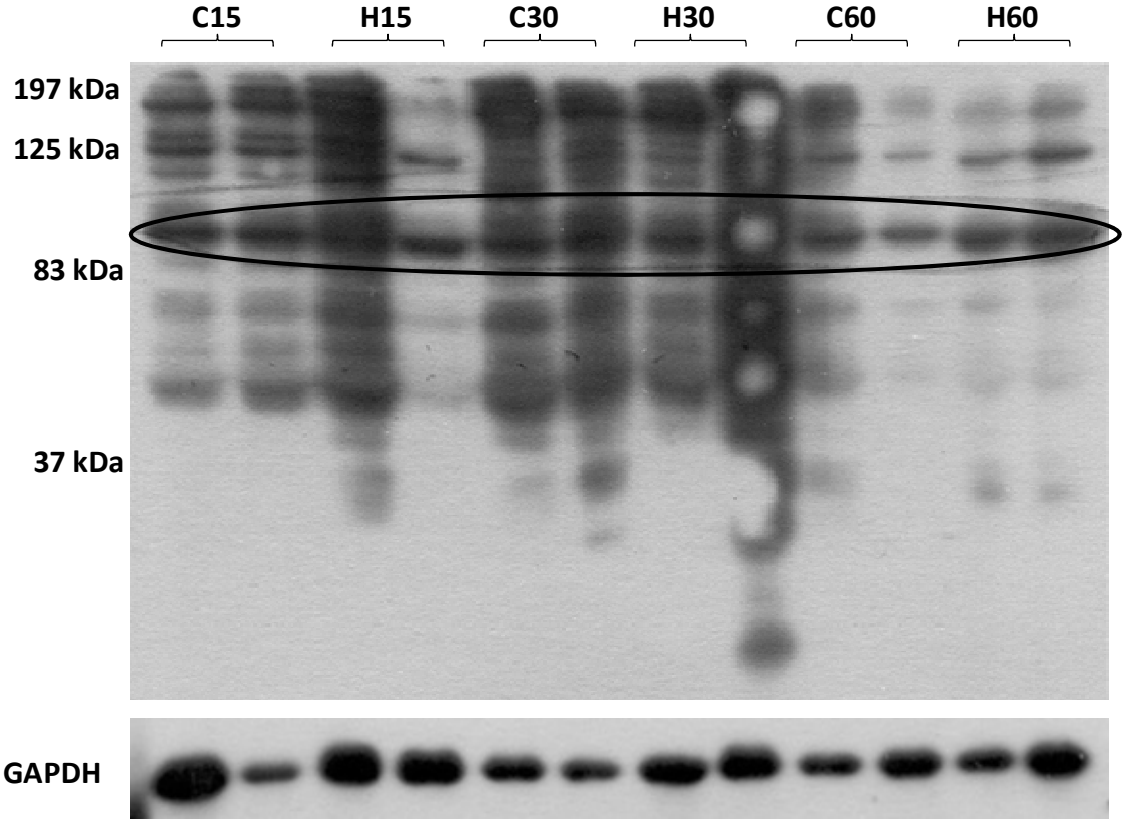
C15
H15
C30
H30
C60
H60
197 kDa
125 kDa
83 kDa
37 kDa
GAPDH

Figure 6.

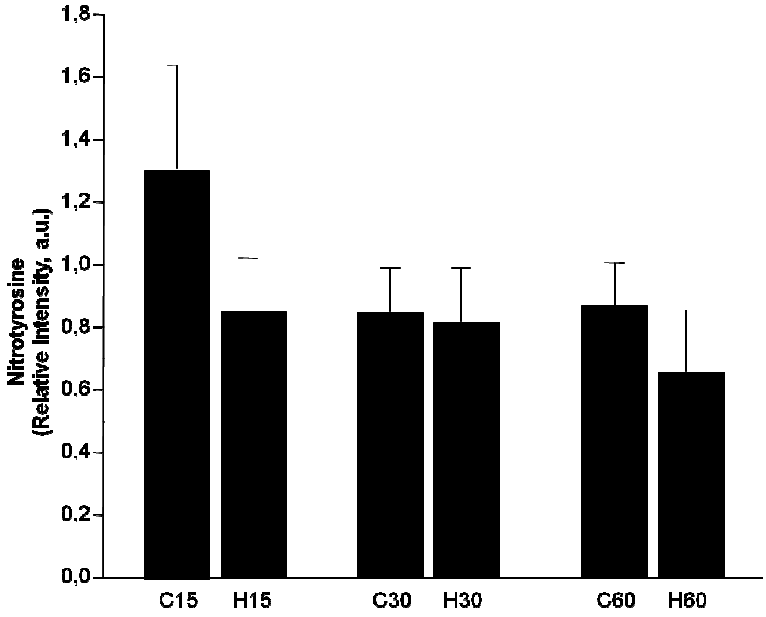
Nitrotyrosine
(Relative Intensity, a.u.)
1,8
1,6
1,4
1,2
1,0
0,8
0,6
0,4
0,2
0,0
C15
H15
C30
H30
C60
H60

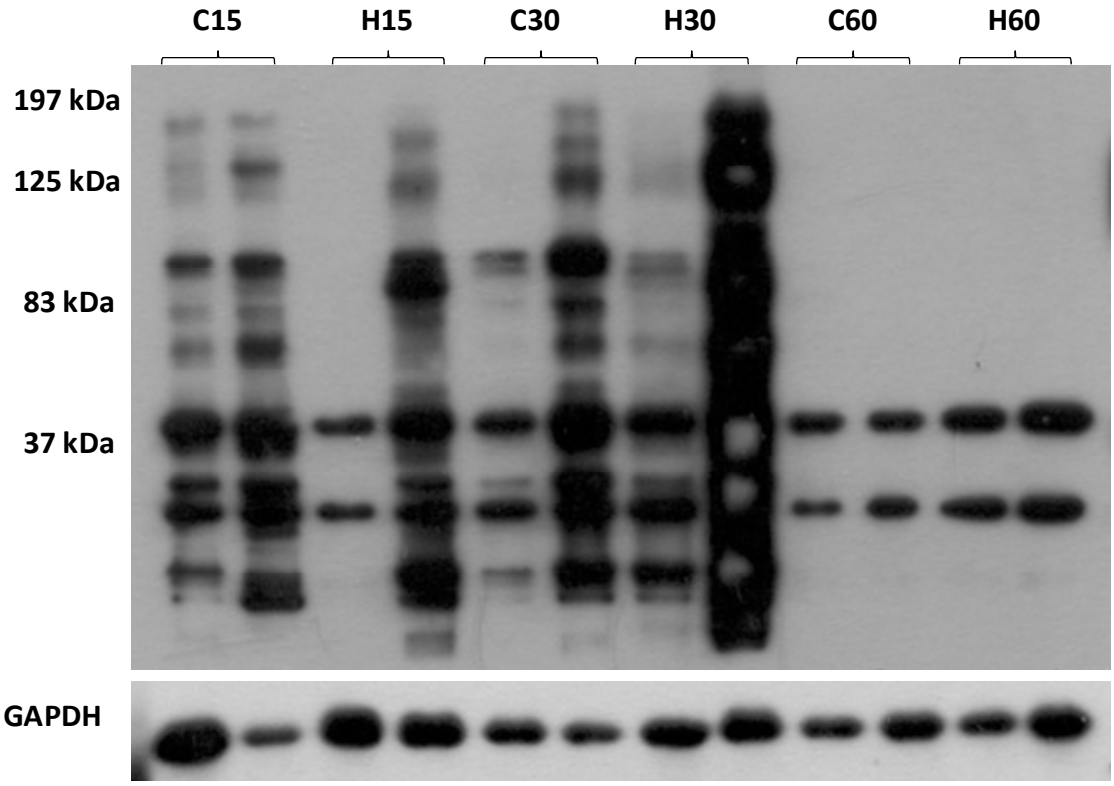
C15
H15
C30
H30
C60
H60
197 kDa
125 kDa
83 kDa
37 kDa
GAPDH

Figure 7A.

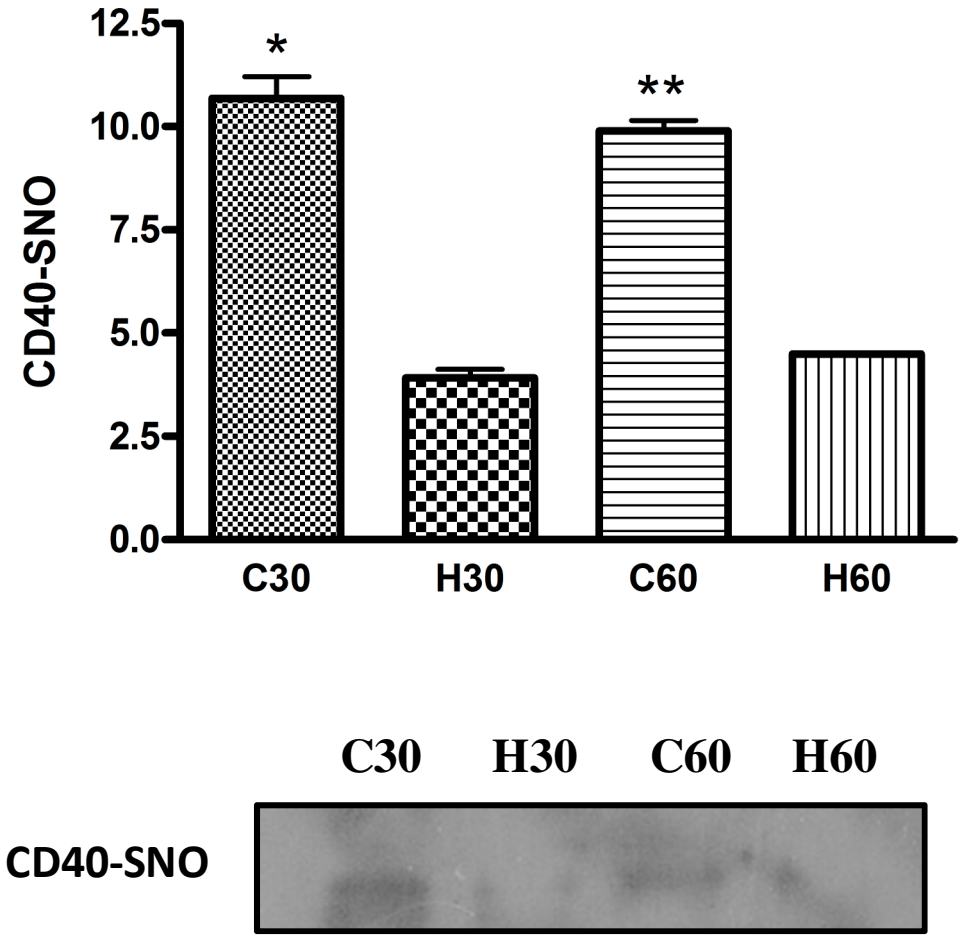
12.5
10.0
7.5
5.0
2.5
0.0
CD40-SNO
*
**
C30
H30
C60
H60
C30
H30
C60
H60
CD40-SNO

Figure 7B.

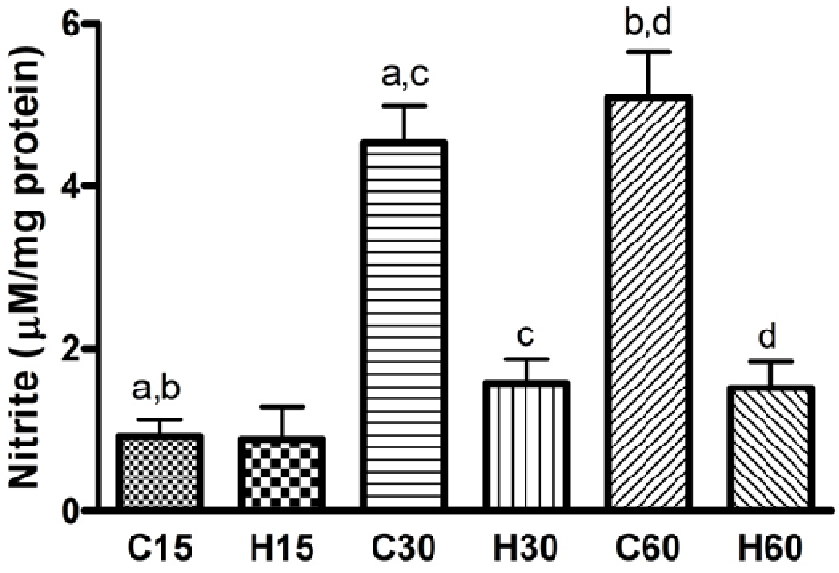

V - CONCLUSÕES

Nossos estudos avaliaram a biodisponibilidade de $NO^{\bullet}$ em função das alterações cardiovasculares, especificamente na hipertrofia ventricular esquerda e aterosclerose, por meio da caracterização das suas vias de síntese/degradação e identificação de seus possíveis alvos demonstraram às seguintes conclusões:

1- A hipertrofia ventricular esquerda (HVE) foi associada ao aumento na geração de H_2O_2 e na morte celular por apoptose.

2- O SNAC mostrou ação cardioprotetora contra o estresse oxidativo por meio da redução de espécies reativas de oxigênio (ROS): H_2O_2 e $O^{-\bullet}_2$.

3- O SNAC induziu a um aumento na expressão e no conteúdo de S-nitrosação do β_2AR e a redução da apoptose. Este processo foi associado ao efeito cardioprotetor à arritmia via indução do acoplamento β_2AR à Gi o qual havíamos descrito anteriormente.

4- A aterogênese inicial em camundongos no curso temporal de 15 a 60 dias foi caracterizada pela progressão do ateroma e este fenômeno não está associada ao aumento nos níveis de dislipidemia e da pressão arterial.

5- O aumento na atividade da eNOS via fosforilação do resíduos de Ser1179 em 30 dias de dieta rica em gordura pode ser considerado como um mecanismo emergencial no combate à aterosclerose e sua redução com a evolução do ateroma em 60 dias em ambas dietas indica o envelhecimento prematuro da vasculatura exposta à aterosclerose.

6- Em 30 e 60 dias de ateroma com indução através de dieta rica em gordura a atividade inflamatória encontrou-se aumentada por meio da denitrosação do receptor CD40. Portanto a análise das alterações no curso temporal apresentou mudanças locais como biodisponibilidade de $NO^{\bullet}$, ativação inflamatória via denitrosação de tióis críticos da via

CD40 e conteúdo de S-nitrosação total, enquanto as mudanças sistêmicas ainda não são evidentes.

DECLARAÇÃO

Declaro para os devidos fins que o conteúdo de minha dissertação/tese de Mestrado/Doutorado intitulada **Biodisponibilidade Cardiovascular do Óxido Nítrico em Camundongos LDLr-/-** .

( ) não se enquadra no § 3º do Artigo 1º da Informação CCPG 01/08, referente a bioética e biossegurança.

(X) tem autorização da(s) seguinte(s) Comissão(ões) de Bioética ou Biossegurança*:
Comissão de Ética no Uso de Animais - CEUA/UNICAMP, sob Protocolo(s) nº2006/04; 2045-1 e 2044-1.

** Caso a Comissão seja externa à UNICAMP, anexar o comprovante de autorização dada ao trabalho. Se a autorização não tiver sido dada diretamente ao trabalho de tese ou dissertação, deverá ser anexado também um comprovante do vínculo do trabalho do aluno com o que constar no documento de autorização apresentado.*

Aluna: Amarylis Claudine Bonito Azeredo Wanschel

Orientadora: Profa. Dra. Marta Helena Krieger

Para uso da Comissão ou Comitê pertinente:
(X) Deferido ( ) Indeferido

Nome:
Função:

Profa. Dra. ANA MARIA A. GUARALDO
Presidente
Comissão de Ética na Experimentação Animal
CEEA/IB - UNICAMP